

## Large alluvial fans on Mars

Jeffrey M. Moore

Space Sciences Division, NASA Ames Research Center, Moffett Field, California, USA

Alan D. Howard

Department of Environmental Sciences, University of Virginia, Charlottesville, Virginia, USA

Received 24 August 2004; revised 30 November 2004; accepted 5 January 2005; published 7 April 2005.

[1] Several dozen distinct alluvial fans, 10 to ~40 km long downslope, have been observed in highlands craters. Within a search region between 0° and 30°S, alluvial fan-containing craters were found only between 18° and 29°S, and they all occur at around ±1 km of the MOLA-defined Martian datum. Within the study area they are not randomly distributed but instead form three distinct clusters. Fans typically descend >1 km from where they disgorge from their alcoves. Longitudinal profiles show that their surfaces are very slightly concave with a mean slope of 2°. Many fans exhibit very long, narrow, low-relief ridges radially oriented downslope, often branching at their distal ends, suggestive of distributaries. Morphometric data for 31 fans were derived from MOLA data and compared with terrestrial fans with high-relief source areas, terrestrial low-gradient alluvial ramps in inactive tectonic settings, and older Martian alluvial ramps along crater floors. The Martian alluvial fans generally fall on the same trends as the terrestrial alluvial fans, whereas the gentler Martian crater floor ramps are similar in gradient to the low-relief terrestrial alluvial surfaces. For a given fan gradient, Martian alluvial fans generally have greater source basin relief than terrestrial fans in active tectonic settings. This suggests that the terrestrial source basins either yield coarser debris or have higher sediment concentrations than their Martian counterparts. Martian fans (and terrestrial Basin and Range fans) have steeper gradients than the older Martian alluvial ramps (and terrestrial low-relief alluvial surfaces), which is consistent with the construction of Martian fans from dominantly gravel-sized sediment (rather than sand and silt). Martian fans are relatively large and of low gradient, similar to terrestrial fluvial fans rather than debris flow fans (although gravity-scaling uncertainties make the flow regime forming Martian fans uncertain). However, evidence of bedforms accentuated by differential erosion, such as scroll bars, supports the contention that these are fluvially formed fans. Martian fans, at least those in Holden crater, apparently formed around the time of the Noachian-Hesperian boundary. We infer that these fans formed during an episode of enhanced precipitation (probably snow) and runoff, which exhibited both sudden onset and termination.

**Citation:** Moore, J. M., and A. D. Howard (2005), Large alluvial fans on Mars, *J. Geophys. Res.*, *110*, E04005, doi:10.1029/2004JE002352.

### 1. Introduction

[2] Alluvial fans are discrete landforms created by the deposition of loose, water-transported material forming broad, gently sloping ramps radiating from mountainous drainage outlets emerging into low-relief basins. They are often found on the Earth along tectonically active mountain-front desert settings where strong relief contrasts and the infrequent precipitation and runoff have prevented the formation of through-flowing drainage systems. When water is available to these drainage basins, it commonly arrives in the form of intense cloudbursts or sudden

snowmelt flash floods. This results in the rapid transport of coarse material, which comes to rest near the drainage outlet both because of the sudden reduction of stream power as it emerges from its confining outlet, and the ephemeral nature of the floods. Successive sheets and lobes of material transported in this manner build up over time to form a fan. The sediment-source drainage basin that feeds a given fan is considered an integral part of the fan system, as the size and shape of the basin, as well as the mechanical properties of the sediment it provides, has a significant effect on a fan's morphology. Fan systems also form in humid climates where there is the juxtaposition of high- and low-relief topography [*Hack*, 1965; *Kochel*, 1990].

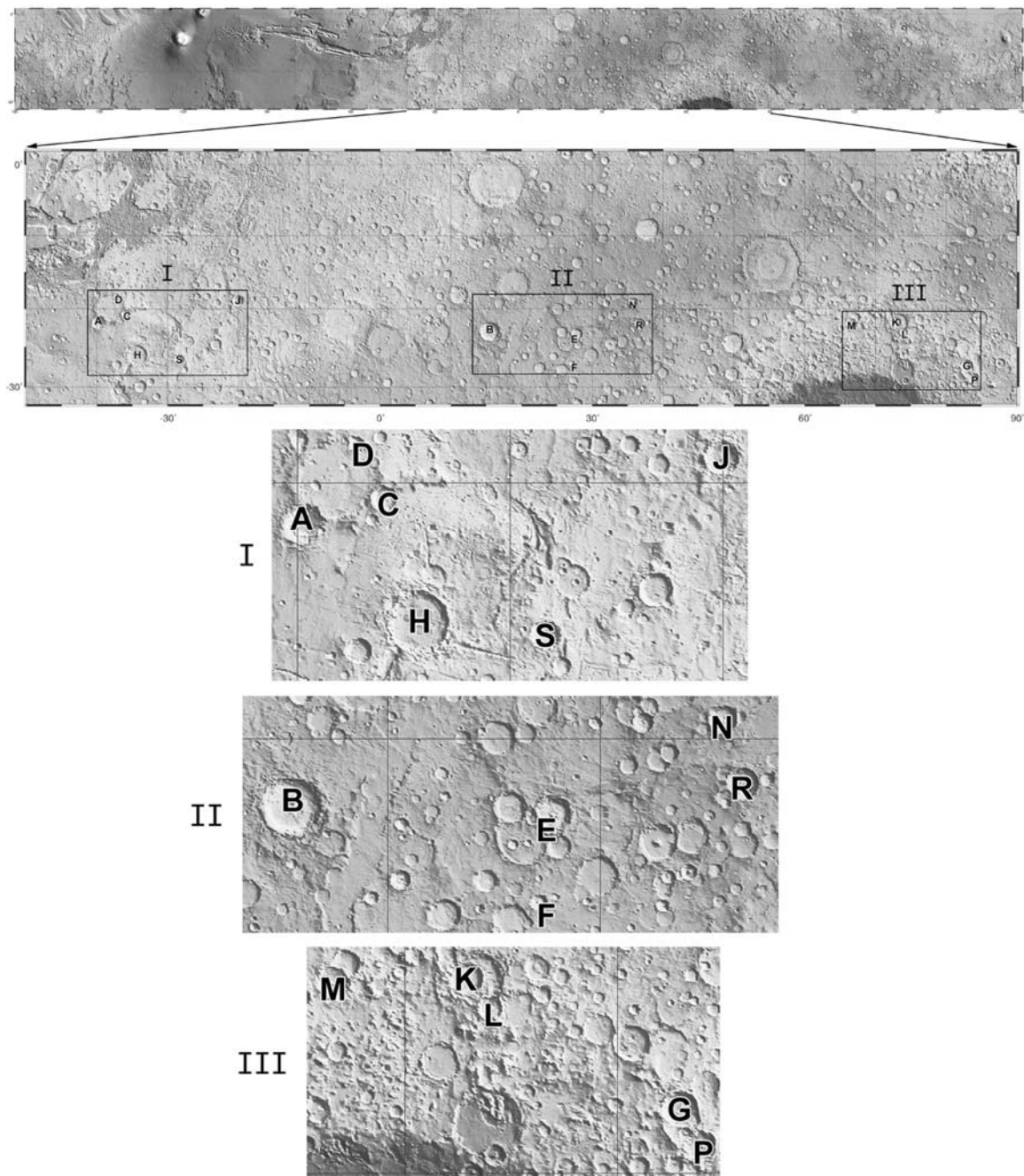


**Figure 1.** Distribution of alluvial fans identified in this study. The uppermost stripe covers all of Mars between the equator and 30°S. The next box down illustrates just the region between 270°W and 60°W. Within the study area, fans are not randomly distributed but instead form three distinct clusters. The lower three boxes show the locations and our identification labels of the fan-containing craters: (I) southern Margaritifer Terra (18–28°S, 18–42°W); (II) southwestern Terra Sabaea (19–28°S, 322–347°W); and (III) southwestern Tyrrhena Terra (21–29°S, 275–294°W) just north of Hellas Planitia. Note that fan site E is actually a three-crater complex in which alcoves share walls (see Figure 11).

[3] Terrestrial alluvial fans have been widely investigated since the later part of the nineteenth century, particularly in the last 50 years, resulting in over 200 peer-reviewed studies. In a historical review, *Lece* [1990] noted that modern fan research initially produced two fan development hypotheses: (1) the evolutionary hypotheses, which held that fans are transient features, forming during early

stages toward landscape maturity, or as part of a long-timescale cycle, akin to a Davisian “geomorphic” cycle [e.g., *Eckis*, 1928; *Lustig*, 1965; *Beaty*, 1970]; and (2) the equilibrium hypothesis, which contended that a state of dynamic equilibrium exists, where the rates of deposition and erosion on fans were essentially equal over some timescale [e.g., *Hack*, 1960; *Denny*, 1965, 1967; *Hooke*,

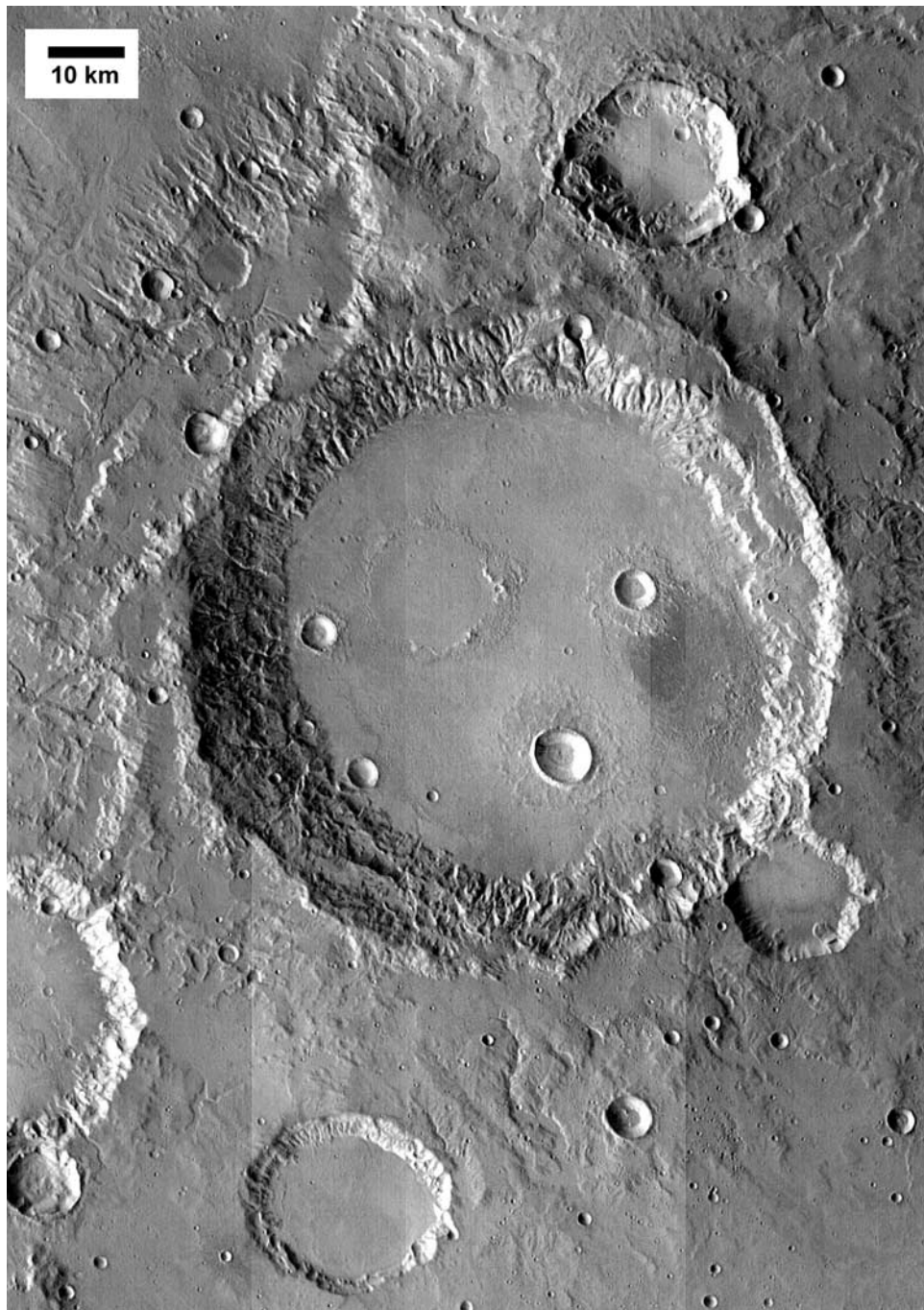


**Figure 2.** Kasimov (centered 24.9°S, 337.1°W, diameter 90 km) and its immediate neighbors are typical examples of degraded craters in the highlands portion of the study area, with Kasimov being the least degraded among those shown here. The vast majority of these craters show some degree of gullying and alcove formation on their rims, but their floors are generally crater-dotted but otherwise featureless plains, and their overall relief is significantly less than that of more pristine craters of the same size. Many craters of this size appear infilled, mantled, and moderately to heavily degraded by smaller impacts.

1968]. The equilibrium hypothesis was nuanced by the recognition that short-timescale fan deposition and erosion rates may fluctuate around a mean condition that itself changes over longer timescales [e.g., Schumm and Lichty, 1965]. It was also recognized that that climatic change and variable tectonic activity complicated the equilibrium hypothesis [e.g., Bull, 1972, 1991]. Modern research has

focused on elucidating the roles of climatic, hydrologic, tectonic and lithologic factors controlling fan development, and moved toward evaluating these individual controls on fan development. Overviews of current research into alluvial fan processes and forms in arid environments are given by Blair and McPherson [1994] and Harvey [1997]. Particularly relevant to this study have been investigations

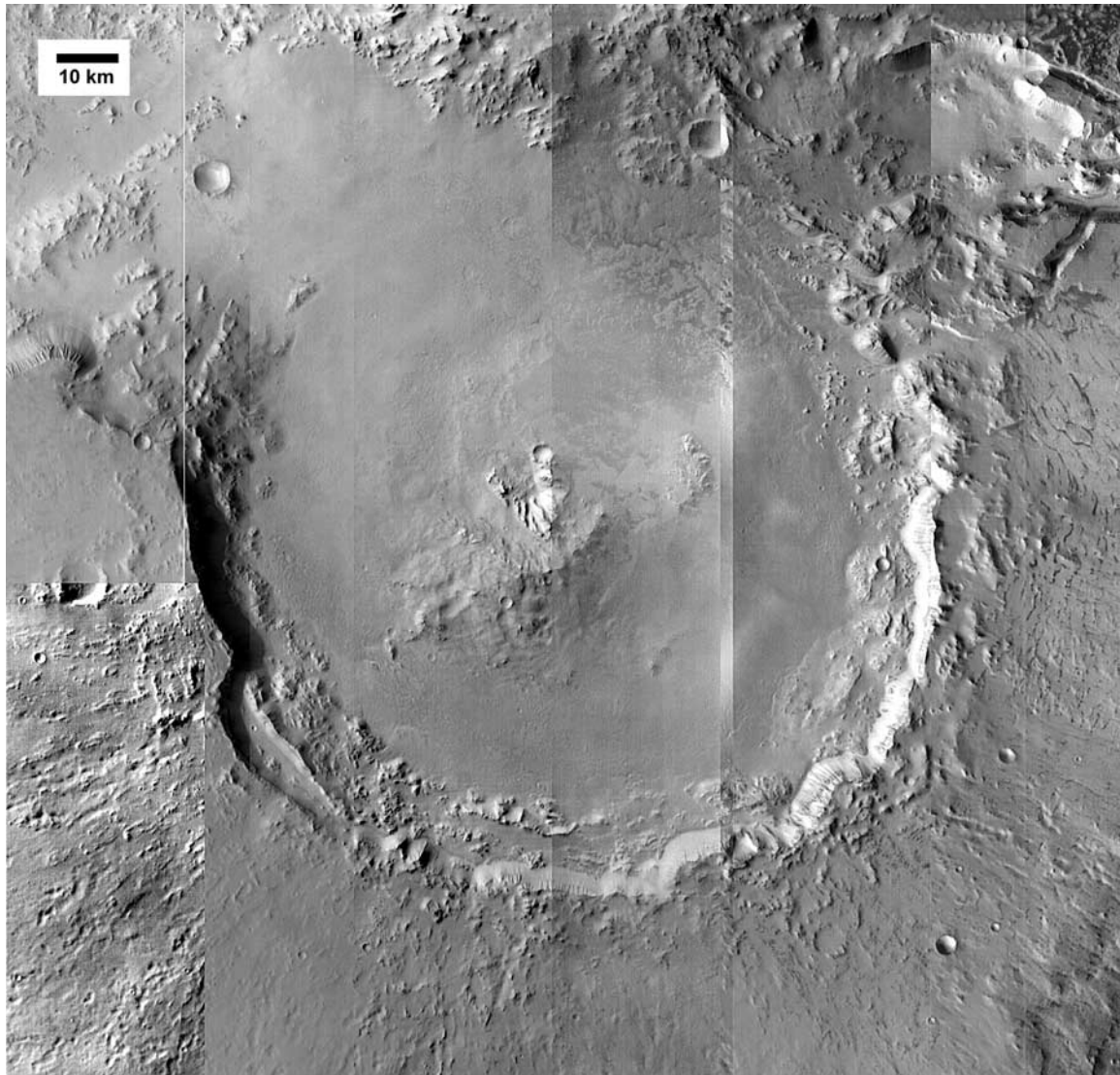


**Figure 3.** Oudemans (centered 10°S, 268°W, diameter 125 km) is the largest example of pristine craters in the study area. Oudemans and four other large craters ( $\geq 70$  km diameter) have very pristine morphologies, including the preservation of small features in their ejecta and floors. They show no sign of fluvial dissection on their rims or alluvial fans on their floors. These fresh craters have terraced rims with, at most, minor talus. Note, however, that the Oudemans floor is mantled presumably by aeolian material, which may be an ongoing process. Also, its northwest wall has been destroyed by the formation of Noctis Labyrinthus.

into the role of the type and size of source sediment in fan morphology [e.g., Bull, 1962; Harvey, 1990], the role of infrequent large-magnitude precipitation and/or flood events [e.g., Beaty, 1974, 1990], and the relationship between source basin morphology and fan properties [e.g., Harvey, 1997].

[4] Although the existence of depositional basins was hypothesized from Viking images [e.g., Goldspiel and Squyres, 1991; Grant, 1987], higher-resolution MOC images and MOLA topography have allowed more definitive characterization of alluvial depositional landforms [e.g., Craddock and Howard, 2002]. Craddock and Howard [2002] noted that Martian degraded crater floors slope toward the crater center with gradients that are lower than alluvial fans in the Basin and Range and Mojave

Desert region, but are equivalent to low-gradient alluvial surfaces and basin fills in humid environments (e.g., the Rocky Mountain-Great Plains transition, fans in the Shenandoah Valley), and alluvial fans in low-relief basins in Arizona and northern Nevada. Craddock and Howard [2002] also reported that MOLA profiles show that a number of isolated massifs are bordered by surfaces sloping away in all directions with gradients typical of terrestrial fans formed of debris shed from adjacent mountains. They argued that while the original shape and size of the massifs is uncertain, the massifs appeared to have been steepened and backwasted by the development of steep, hierarchical valleys with debris from these massifs apparently spreading into alluvial fans radiating from the massifs.

**Table 1.** Sizes and Locations of Alluvial Fans Bearing Craters Identified by This Study

Label	Name	Diameter, km	Latitude, S	Longitude, <sup>a</sup> E
A	none	99	22.11	320.55
B	Bakhuysen	157	23.21	15.82
C	none	69	20.65	324.28
D	none	37	18.25	323
E(north)	none	92	23.61	28.02
E(west)	none	27	23.47	27.05
E(south)	none	58	24.65	28.28
F	none	50	27	27.3
G	none	90	27.59	83.26
H	Holden	145	26.31	326.09
J	Jones	89	19.11	340.29
K	none	84	22.08	73.18
L	none	60	23	74.2
M	none	83	22.16	66.94
N	none	78	19.42	36.03
P	none	75	29.1	84.24
R	none	82	22.31	36.91
S	Ostrov	75	26.85	331.92

<sup>a</sup>Note: In this paper, E longitude denotes the use of a planetocentric coordinate system, whereas W longitude denotes the use of a planetographic coordinate system.

[5] In addition to a preliminary report [Moore and Howard, 2004] of the alluvial fans examined in this study, there have been several other recent investigations that have touched on Martian alluvial fans. Crumpler and Tanaka [2003], in geologic mapping of the mountainous southern rim (Libya Montes) of Isidis Planitia, interpreted dissected ramps of material descending from the flanks of massifs and ridges into intermontane plains, which they give the

name “fluted and dissected material,” as alluvial fans. It had been suggested that ramps, mesas and knobs situated in craters where inflowing valleys breach crater walls could be alluvial fans or deltas on the basis of studies of Viking orbiter images [Cabrol and Grin, 2001], but due to the resolution and topographic limitations of the data, such interpretations could not be verified by evidence of unambiguously fluvial channels or fluvial stratigraphy on these

**Table 2.** Geomorphic Data and Locations of 31 Alluvial Fans Used for Statistics in Figures 12–17

Fan Label (Name)	Profile Location	Apex Latitude	Apex Longitude, <sup>a</sup> E	Catchment Size, km <sup>2</sup>	Catchment Relief, km	Catchment Gradient, deg	Fan Size, km <sup>2</sup>	Fan Relief, km	Fan Gradient, degrees	Fan Length, km	Fan Concavity, km <sup>-1</sup>
A1		-21.14	320.66	170	1.9	6.4	516	1.24	1.83	38.7	0.0237
A2	W	-21.52	320.09	147	2.7	7.33	114	0.8	2.03	22.6	0.0717
C1	N	-20.34	324.21	220	2.2	9.14	226	0.3	1.3	13.2	0.0197
D1	NW	-18.09	322.89	161	1.5	5.62	65	0.4	2.66	8.6	0.0819
D2	SE	-18.41	323.25	48	0.9	8.96	41	0.7	5.67	7.0	0.1850
E1	N	-23.91	28.15	170	1.3	3.62	526	0.8	2.08	22.0	0.0215
E2	S	-24.31	28.29	101	0.9	4.16	396	0.76	1.67	26.1	0.0441
E3	W	-23.62	27.18	23	0.9	5.74	70	0.36	2.56	8.1	0.1112
E4	NW	-24.84	27.42	135	1.7	3.57	207	0.7	2.16	18.5	0.0656
E5	WN	-23.32	27.07	103	1.35	7.04	114	0.45	2.58	10.0	0.0574
E6	W to E	-23.56	27.44	89	1	4.87	236	0.6	2.08	16.5	0.0444
H1	N	-24.96	325.71	162	1.4	3.62	634	1	1.52	37.7	0.0205
H2	SW	-26.43	324.84	139	2.1	8.18	231	1	2.53	22.6	0.0230
H3	W	-25.88	324.85	408	1.8	4.51	372	1.2	2.66	25.8	0.0297
J1		-18.32	340.11	53	1.8	9.29	326	0.9	2.21	23.3	0.0375
K1	NW	-21.35	72.68	255	1.5	5.51	520	1.2	1.82	37.9	0.0193
K2	W	-21.66	72.56	340	2.3	5.06	564	1.1	1.82	34.5	0.0045
L1		-22.73	74.46	126	1.8	5.8	370	0.66	2.23	16.9	0.0626
L2	E	-23.04	74.74	34	0.9	9.81	46	0.48	3.21	8.6	0.1344
L3	NW	-22.76	74.03	159	0.9	3.53	130	0.2	1.42	8.0	0.0297
L4	S	-23.45	74.35	145	1.3	5.6	225	0.6	1.96	17.5	0.0593
L5	SE	-23.37	74.58	112	1.65	7.09	141	0.55	2.33	13.5	0.0653
L6	SW1	-23.31	73.99	30	2.2	12.17	29	0.4	3.59	6.4	0.3151
L7	SW2	-23.14	73.83	113	1.2	10.82	84	0.6	3.6	9.5	0.1445
M1		-21.47	67.22	108	1	6.02	405	0.5	1.48	19.3	0.0416
M2	NW	-21.68	66.41	90	2.3	8	126	0.6	2.25	15.2	0.2295
M3	SW	-22.36	66.53	84	1.9	8.56	177	0.9	3.24	15.9	0.0602
P1	N	-28.49	84.07	308	1.7	6.02	310	0.7	1.77	22.7	0.0368
P2	NE	-28.54	84.51	177	1.8	9.05	256	1.3	3.21	23.2	0.0392
S1	NE	-26.23	331.52	195	1.4	6.12	153	0.6	2.1	16.4	0.0351
S2	S	-27.00	331.99	210	1.3	6.76	181	0.6	2.33	14.8	0.0551

<sup>a</sup>Note: In this paper, E longitude denotes the use of a planetocentric coordinate system, whereas W longitude denotes the use of a planetographic coordinate system.

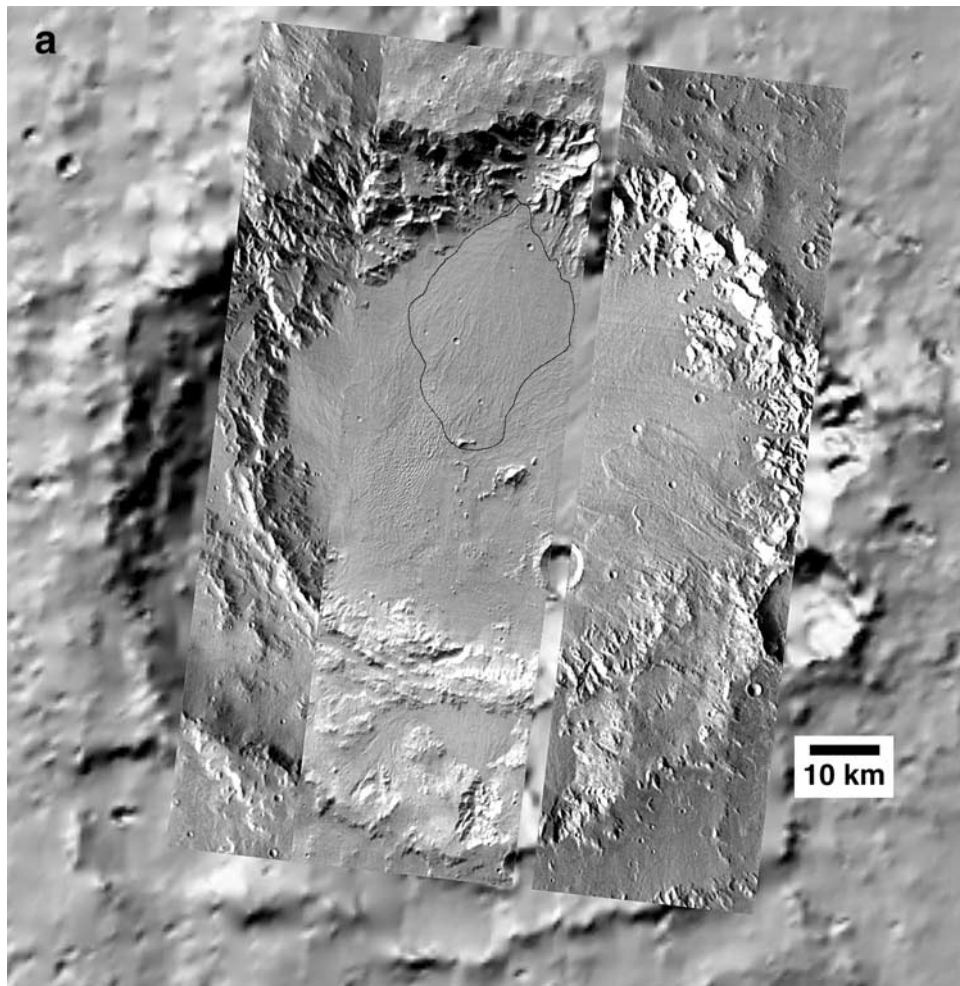


**Figure 4.** (a) A typical example of a fan in this study. The fan (A1, outlined) occurs in 99-km-diameter crater A (centered  $19.5^{\circ}\text{S}$ ,  $39.5^{\circ}\text{W}$ ), which contains several other fans. The A1 fan appears to have had the last active deposition within this crater, as its periphery superposes all others. (b) Nighttime THEMIS IR images of the fan A1 indicate that these ridges are warmer and thus have a relatively higher thermal inertia than their surroundings, implying that they are composed of coarser or more indurated material than the material immediately surrounding them. Nighttime IR images of other fans indicated that this is common. (c) A longitudinal profile of fan A1 shows that its surface is very slightly concave with an average slope of  $2^{\circ}$  over a downslope distance of  $\sim 40$  km. (d) MOLA-derived topographic map of crater A showing the locations of fans A1 and A2. Map is 135 km wide; contour interval is 50 m.

landforms. On the basis of high-resolution MOC images, *Malin and Edgett* [2003] and *Moore et al.* [2003] describe and analyze an alluvial delta (located at  $24.1^{\circ}\text{S}$ ,  $33.9^{\circ}\text{W}$ , within a crater provisionally named Eberswalde) and its drainage system, citing it as the first unambiguous evidence for fluvial, layered deposits on Mars. *Pondrelli et al.* [2004], in an abstract postulating the evolution of Martian paleolacustrine systems, noted, as did *Moore and Howard* [2004], the presence of large alluvial fans in Holden crater. In a separate abstract to the same conference, *Williams et al.* [2004] discussed numerous pristine, uncratered, km-scale features interpreted to be alluvial fans found along the inner rim of a  $\sim 60$  km-diameter crater provisionally named “Mojave” ( $7.6^{\circ}\text{N}$ ,  $33.0^{\circ}\text{W}$ ); such features had not been observed elsewhere on Mars. This study describes the morphology, setting, age range, and other remotely sensed characteristics of a class of alluvial fans on Mars that are

older and larger ( $>10$  km long) than those described by *Williams et al.* [2004]. We produce statistical analysis of several morphometric aspects of these fans and compare them to analogous statistics for terrestrial fans. We discuss the amounts and rates of water necessary to create these fans and the types and size of source sediment. We speculate on the implications of their geographical and temporal range limits. Finally, we discuss what these fans may imply about the Martian climate at the time of their emplacement.

## 2. Observations

### 2.1. Geologic Setting

[6] The alluvial fans investigated in this study were initially recognized in  $\sim 100$  m/pixel daytime thermal infrared (IR) Thermal Emission Imaging System (THEMIS) images

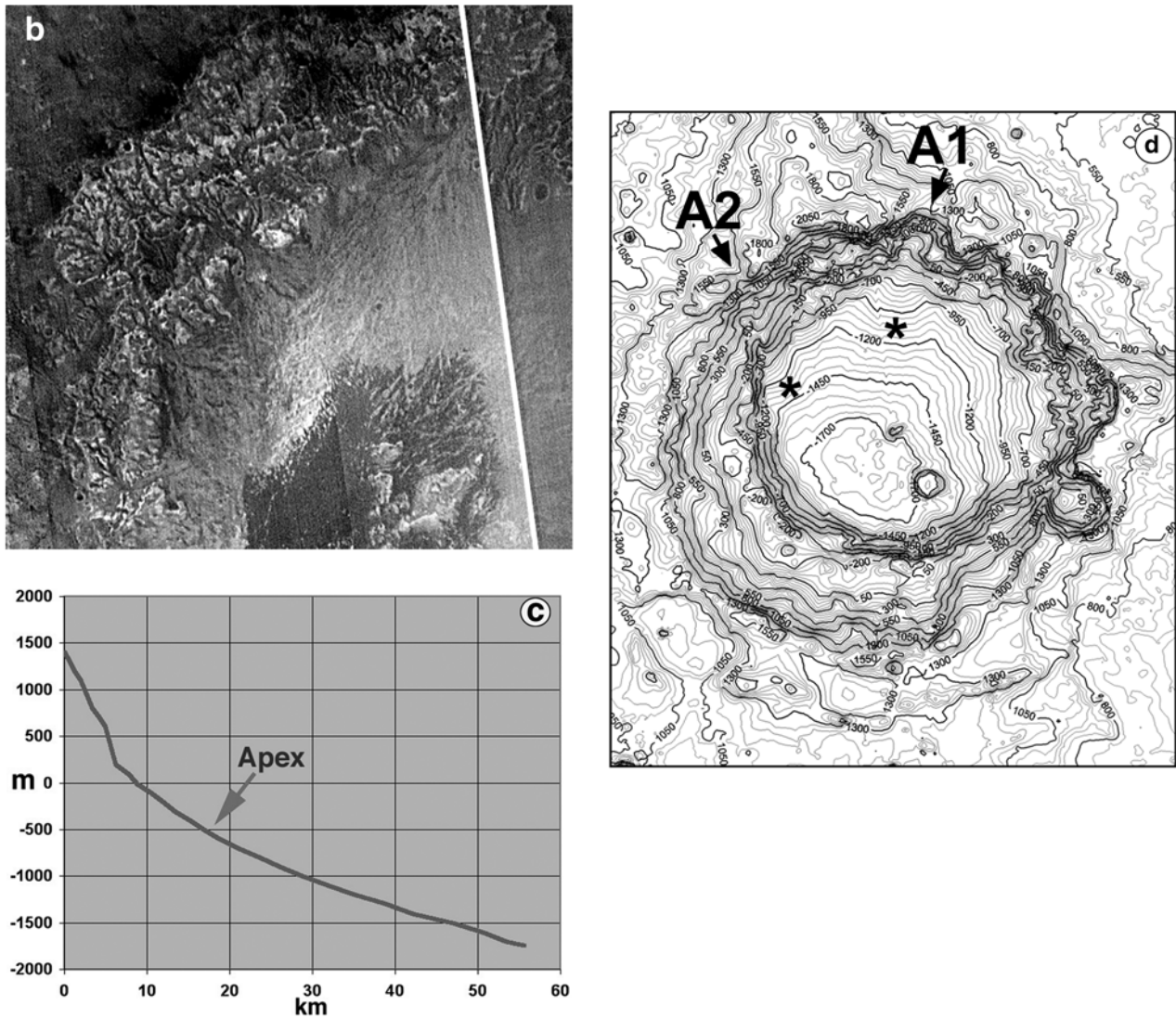
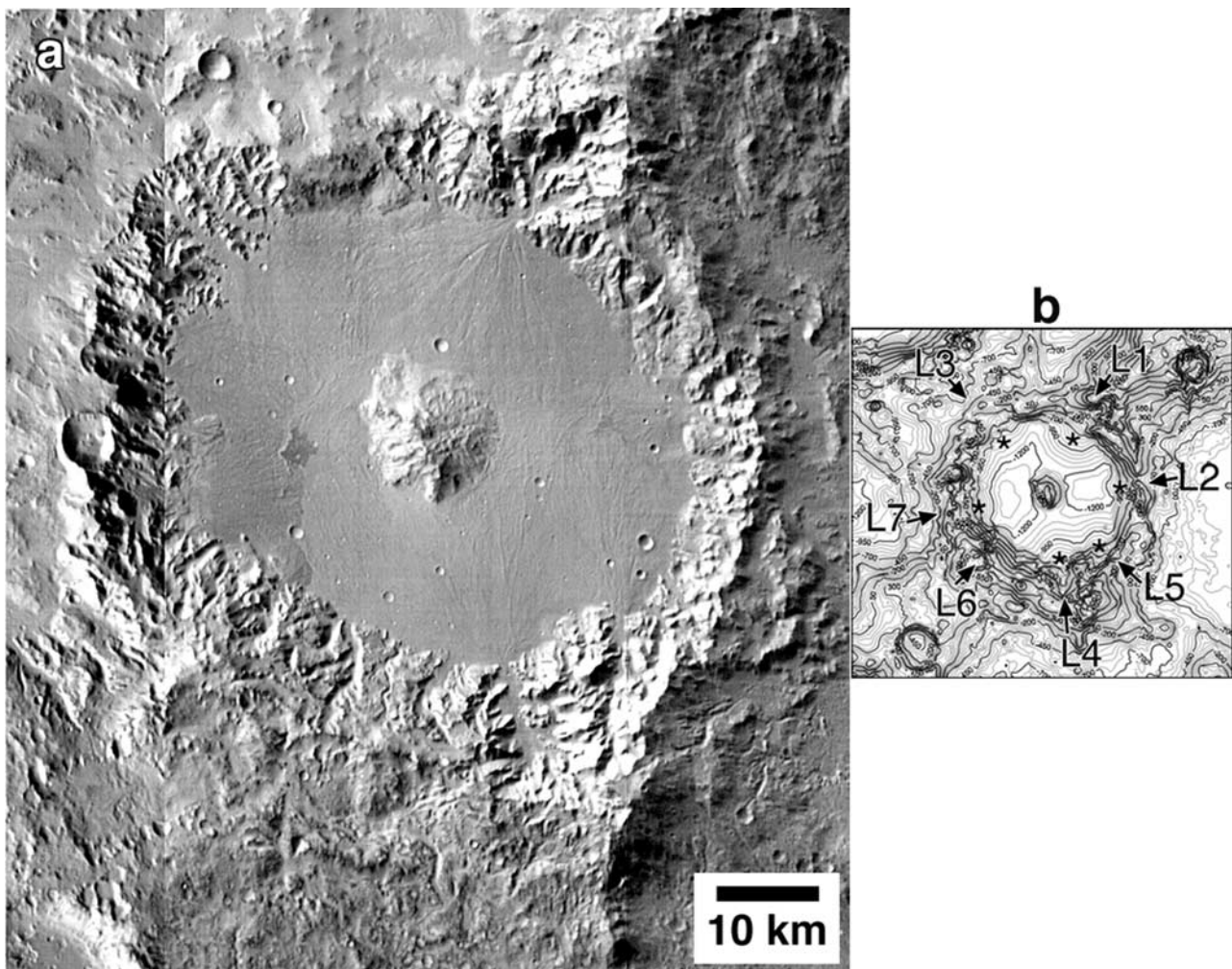


Figure 4. (continued)

we have been systematically surveying as part of a broader study of highlands basins and their deposits [e.g., Moore *et al.*, 2003; Howard and Moore, 2004a]. The size, their grossly undulate shape, and the fine-scale textures on the fans studied here prevented their recognition in earlier lower-resolution comprehensive coverage from either the Viking orbiter cameras or the Mars Global Surveyor (MGS) Mars Orbiter Camera (MOC) wide-angle (WA) “geodetic” survey. There is some coverage of these fans in MOC narrow-angle (NA) images and in THEMIS  $\sim 20$  m/pixel visible light (VIS) images, which are useful for texture studies once the fans are recognized in the THEMIS IR coverage. The fans of this study are, for the most part, large enough to have been adequately sampled by the Mars Orbiter Laser Altimeter (MOLA) aboard MGS, which we have extensively utilized for our topographic descriptions and analysis of these features. It is the combination of THEMIS daytime IR images and MOLA topography that makes the interpretation of these features as alluvial fans unambiguous.

[7] Using available THEMIS daytime IR images (as of April 2004), we systematically surveyed all of Mars between the latitude of  $30^{\circ}\text{S}$  and the equator for alluvial fans. We limited ourselves to this latitude band because heavily cratered terrain in the Northern Hemisphere (Arabia) is pervasively mantled [e.g., Christensen, 1986; Moore, 1990]. Likewise terrain southward of  $30^{\circ}\text{S}$  was not examined because of the onset of the pervasive Amazonian mantle [e.g., Soderblom *et al.*, 1973; Head *et al.*, 2003]. All the alluvial fans we found were within 18 craters, mostly larger than 60 km in diameter (the 3 exceptions being craters 38, 30 and 23 km in diameter) containing recognizable alluvial fans (Figure 1). Alluvial fan-containing craters were found only between  $18^{\circ}$  and  $29^{\circ}\text{S}$ , and they all occur at around  $\pm 1$  km of the MOLA-defined Martian datum. Within the study area they are not randomly distributed but instead form three distinct clusters: (1) southern Margaritifer Terra ( $18\text{--}28^{\circ}\text{S}$ ,  $18\text{--}32^{\circ}\text{W}$ ); (2) southwestern Terra Sabaea ( $19\text{--}28^{\circ}\text{S}$ ,  $322\text{--}347^{\circ}\text{W}$ ); and (3) southwestern Tyrrhena Terra ( $21\text{--}29^{\circ}\text{S}$ ,  $276\text{--}294^{\circ}\text{W}$ ) just north of Hellas Planitia.



**Figure 5.** (a) Crater L (diameter 66 km, centered on 23.5°S, 285.7°W), whose floor is covered by alluvial fans (except for the central peak). (b) MOLA-derived topographic map of crater L showing the locations of fans L1 and L4, among others. Map is 125 km wide; contour interval is 50 m. North is up for all.

[8] In order to evaluate the frequency and distribution of alluvial fans in craters, we started with the 218 craters between 500 and 70 km in diameter identified in the *Catalog of Large Martian Impact Craters* (N. G. Barlow, submitted as NASA Contractor Report, 1987). In the study latitude band, of which 138 of them were sufficiently imaged by July, 2004, to evaluate for the presence of alluvial fans. The vast majority of these craters show some degree of gullying and alcove formation on their rims, but their floors are generally crater-dotted but otherwise featureless plains, and their overall relief is significantly less than that of more pristine craters of the same size. Many craters of this size appear infilled, mantled, and moderately to heavily degraded by smaller impacts. Kasimov (centered 24.9°S, 337.1°W, diameter 90 km) and its immediate neighbors are typical examples of these degraded craters, with Kasimov being the least degraded among those shown in Figure 2. The 15 craters in this sample that did possess alluvial fans are generally less infilled, mantled and degraded and exhibited greater relief than craters devoid of discrete recognizable fans. However there are five large craters ( $\geq 70$  km diameter) that have very pristine mor-

phologies including the preservation of small features in their ejecta and floors. They show no sign of fluvial dissection on their rims or alluvial fans on their floors. These fresh craters have terraced rims with, at most, minor talus. Oudemans (centered 10°S, 268°W, diameter 125 km) is the largest example of these pristine craters (Figure 3). These observations suggest that the fans predate the most recent and pristine large Martian impact craters, but they are also rare on highly degraded impact craters. We speculate that the low rim relief of highly degraded Noachian craters prevented alcove erosion and fan formation, but a few late Noachian impact craters retained rims of sufficient steepness and height for fan formation during an intermediate time period on Mars (possibly at the Noachian-Hesperian boundary, as we discuss below).

## 2.2. Alluvial Fans and Their Host Craters

[9] Most of the craters in which alluvial fans are found have not been named. Therefore we have given these craters arbitrary letter designations (Figure 1, Table 1). The few fan-containing craters with names were given letter designations based on the first or second letter in their name.



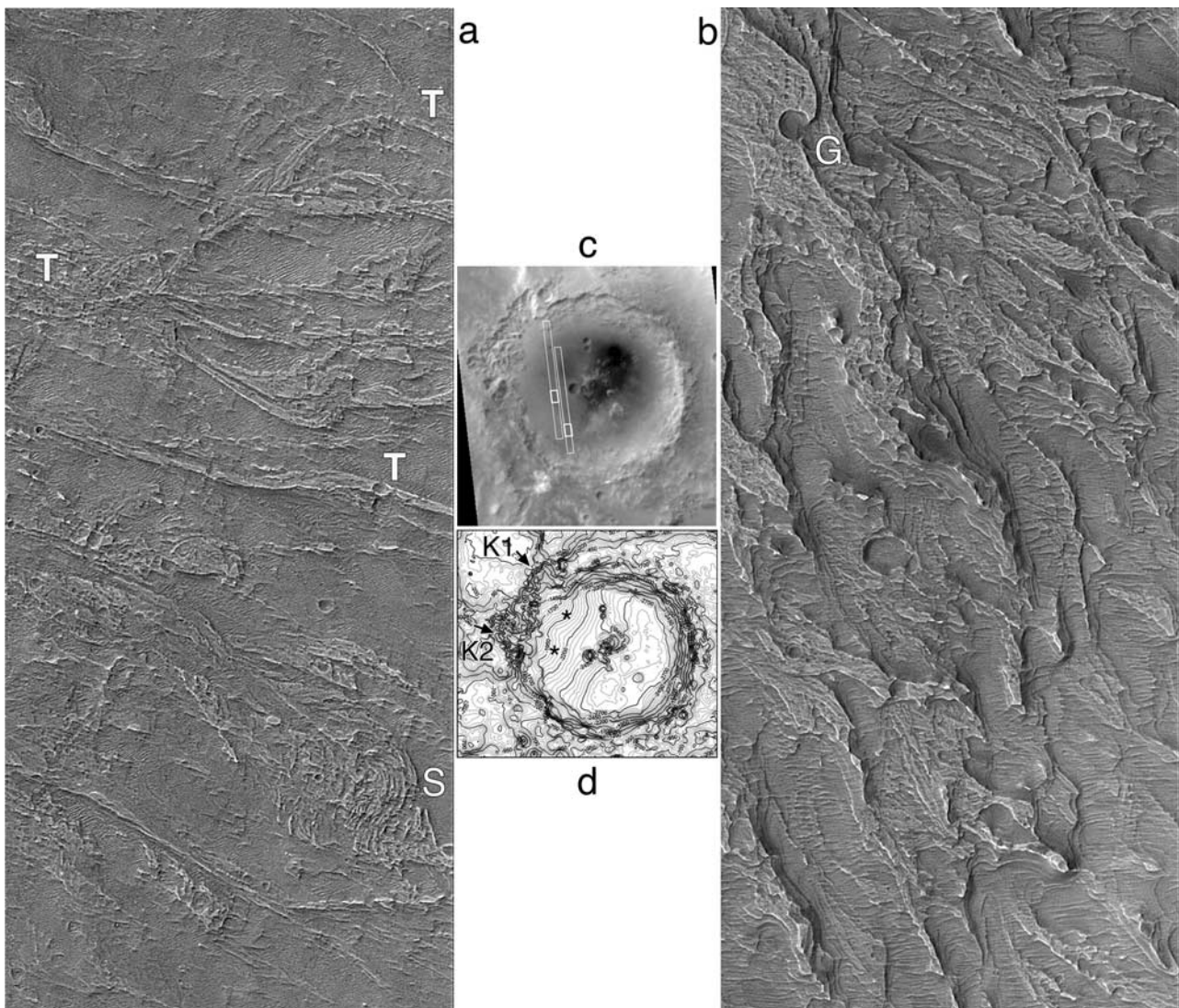


**Figure 6.** High-resolution view of fan surfaces. These excerpts from MOC NA images R15-01087 (left, original resolution 4.5 m/pixel, image width is 2.9 km) and R15-01806 (right, original resolution 4.4 m/pixel, image width is 3.0 km) reveal details on fan K2. These images show differentially eroded fan deposits where erosion-resistant gravel center beds are exposed after finer side-bed material had been removed. In Figure 6a, note ridge sets interpreted to be scroll bars (immediately left of S), and finely digitate distributaries (bounded within the area marked with the letters T). Figure 6b exhibits low, broad, flat-topped, sinuous-sided ridges interpreted to be terminal gravel sheets (immediately left of G) seen near the fan periphery, all supportive of the hypothesis that the fans were fluvial rather than debris fed. Figure 6c provides context for the MOC NA images, roughly centered on 22°S, 287°W: Figure 6a on the left and Figure 6b on the right. Illumination is from the west in all three images. Figure 6d is a MOLA-derived topographic map of crater K showing the location of fan K2, among others. Map is 120 km wide; contour interval is 50 m. North is up for all.

Likewise, individual fans evaluated in this study were given a number, which combined with the host crater letter, uniquely identifies them (Table 2). Thirty-one representative fans in the 18 craters were selected for measurements of morphometry using MOLA data (Table 2). The primary criterion for selection was the ease of recognition in images and MOLA data of the contributing upland basin and lateral and terminal fan boundaries.

[10] All fans in this study issue from, steep-walled scalloped alcoves and rarely is there evidence for flow from beyond the crater rim into alcove heads, indicating the

fans are usually composed of the material eroded to form the alcove, and the alcove *is* the catchment. A typical example of a fan in this study is shown in Figure 4. The fan (A1) occurs in 99-km-diameter crater A (centered 19.5°S, 39.5°W), which contains several other fans. The A1 fan appears to have had the last active deposition within this crater, as its periphery superposes all others. Crater A has an interior ~70-km-diameter flat-floored depression offset to the north ~10 km predating the fans that probably is another impact crater that excavated into the 99-km-diameter basin. The superposition resulted in an anomalous

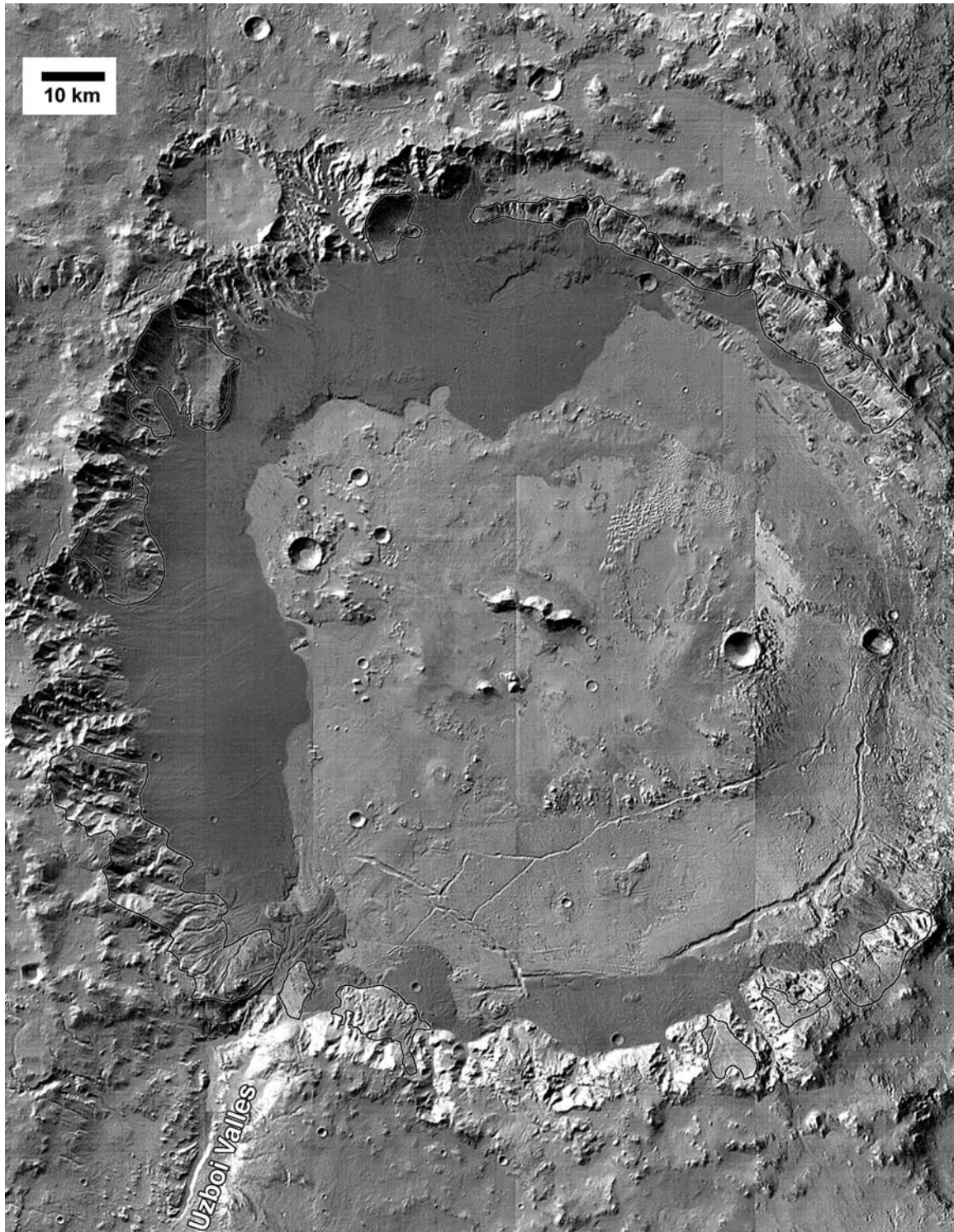


**Figure 7.** Holden crater (145-km-diameter, centered 26.3°S, 33.9°W) contains large, numerous alluvial fans (shaded), which are laterally integrated into a bajada complex and have interacted with an apparent fluvial-lacustrine system fed by Uzboi Valles that entered on the southwest side of Holden and exited through a breach in the eastern wall. Locally, highly dissected terrain (outlined) at the foot of the crater wall appears to define an early stage of fan deposition, which was subsequently eroded during later fan emplacement.

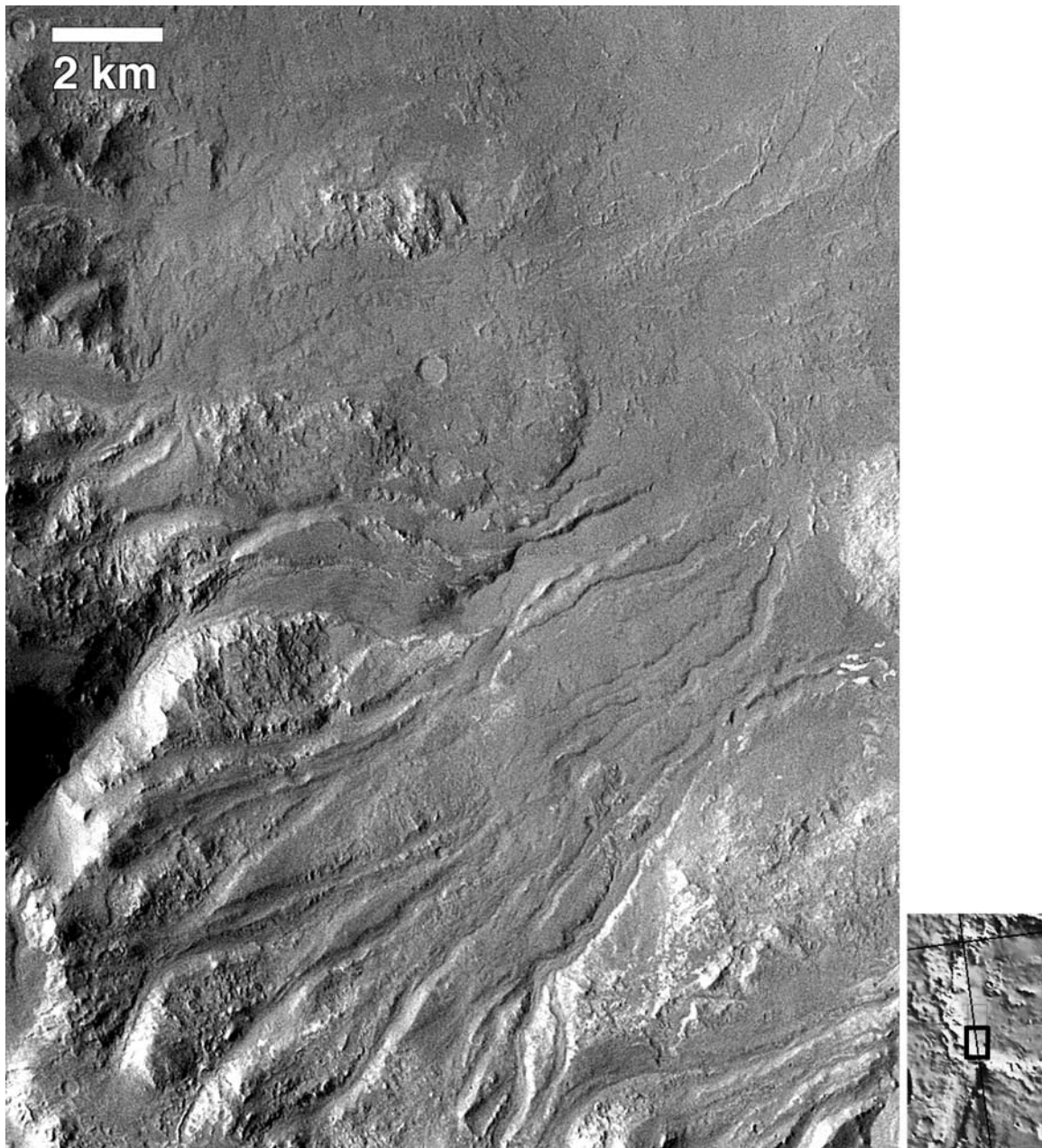


**Figure 8.** Several fanheads of alluvial fans in Holden, near the entrance of Uzboi Vallis, are dissected by flat-floored channels. One main fanhead trench, in the upper half of the image, branches into a network of distributary channels. The formation of prominent fan head entrenchment on the Holden fans may be the response to removal of material from their lowest peripheries [e.g., Mack and Leeder, 1998]. (THEMIS VIS image V01762003; inset shows context for the original image, centered 26.49°S, 34.97°W, and the portion of that image shown here. North is up. Illumination is from the west.)

steeper and deeper north rim of the basin complex where the fans occur. The southeast rim of crater A is altered by a 16-km-diameter crater whose ejecta covers, and thus post-dates, all the fans in crater A. Crater A's own ejecta is cut by secondary craters from 140-km-diameter Holden located ~380 km to the southeast. The alcove of A1 is ~10 km long downslope and ~15 km wide across its spur-and-gullied back walls. These back walls have ~1 km relief and typically slope ~15°. Fan A1 exhibits the classic tear shape in plan view, some 25 km at its widest point. The fan

descends some ~1250 m from where it discharges from the alcove (i.e., at the apex). A longitudinal profile of fan A1 shows that its surface is very slightly concave with an average slope of 2° over a downslope distance of ~40 km (Figure 4c). The distal portion (or toe) of this fan is partially covered by a dune field. Fan A1 exhibits very long, narrow low-relief ridges radially oriented downslope, often branching at their distal ends. We interpret these ridges to be remnants of the distributary channel system of the fan. Nighttime THEMIS IR images of the fan A1

(Figure 4b) indicate that these ridges are warmer and thus have a relatively higher thermal inertia than their surroundings, implying that they are composed of coarser or more indurated material than the material immediately surrounding them. Nighttime IR images of other fans indicated that this is common. Notably missing from this and all other Martian fans of this investigation are the small, surficial,

often branching gullies found on terrestrial fans caused by precipitation and runoff acting directly on the fans themselves and completely unassociated with flow from the fans' superjacent catchment. Alluvial fan deposits cover their hosts' crater floors up to the end-member state represented by 66-km-diameter crater L (centered 23.0°S, 285.7°W), whose floor is completely covered exclusive of the central

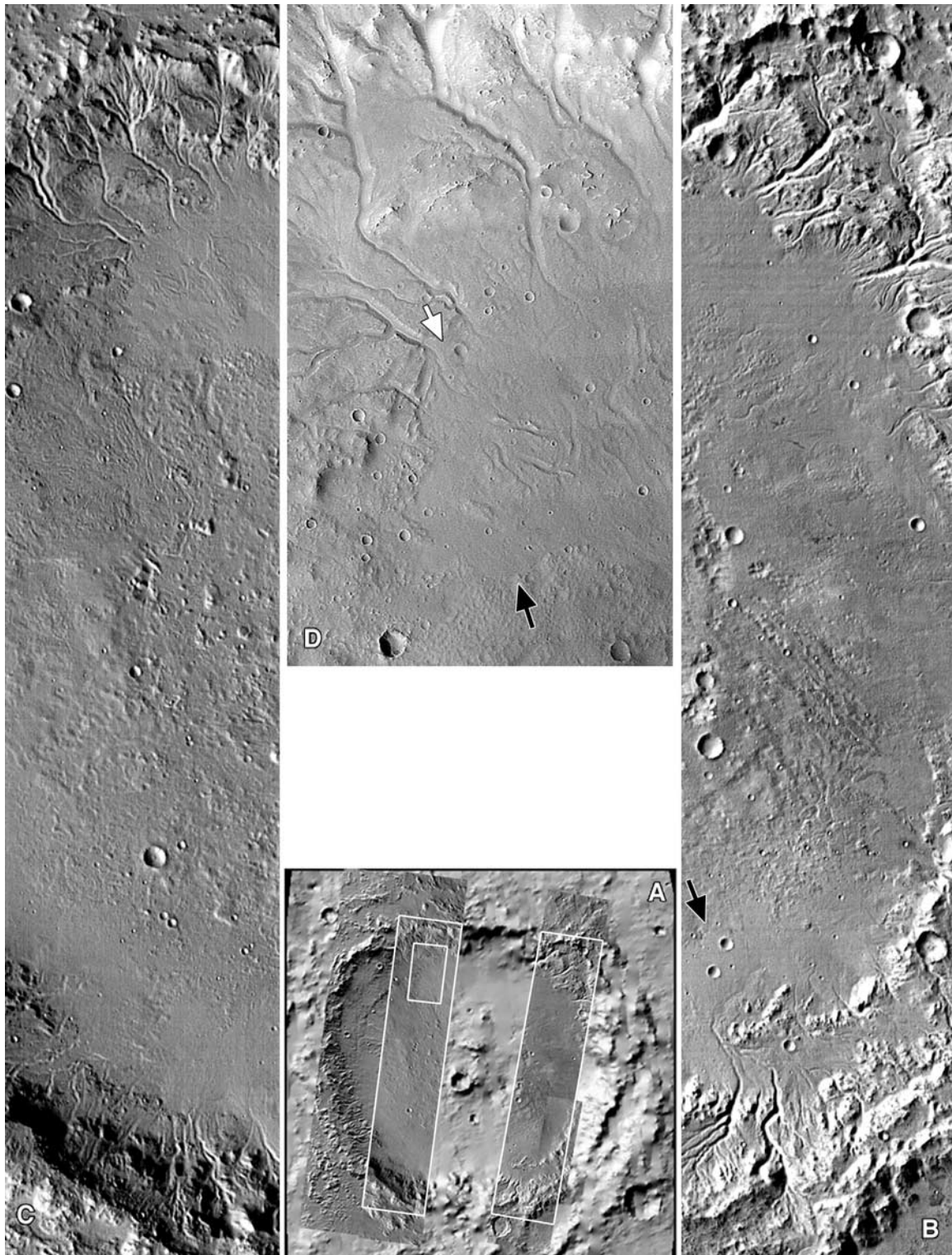
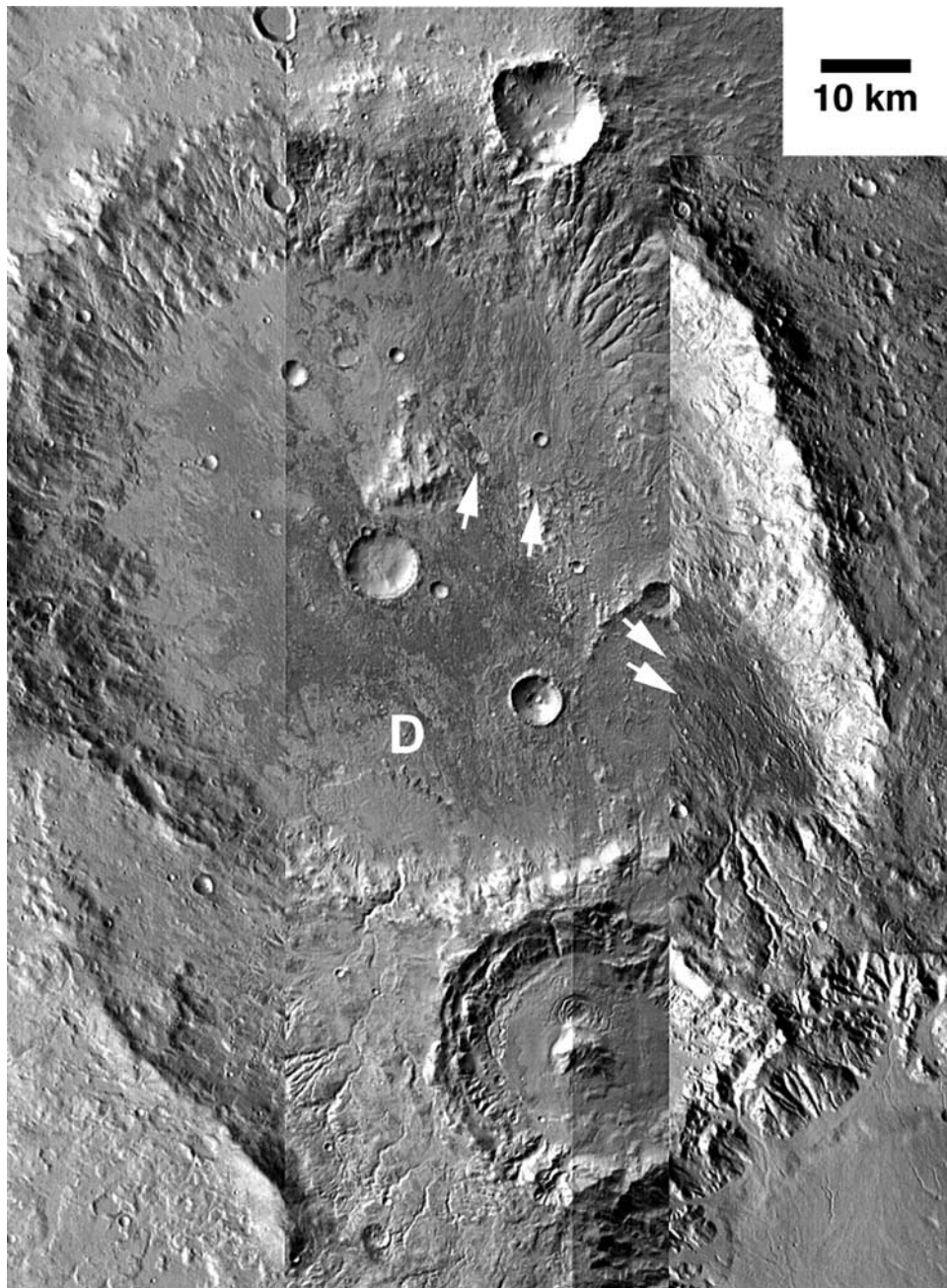
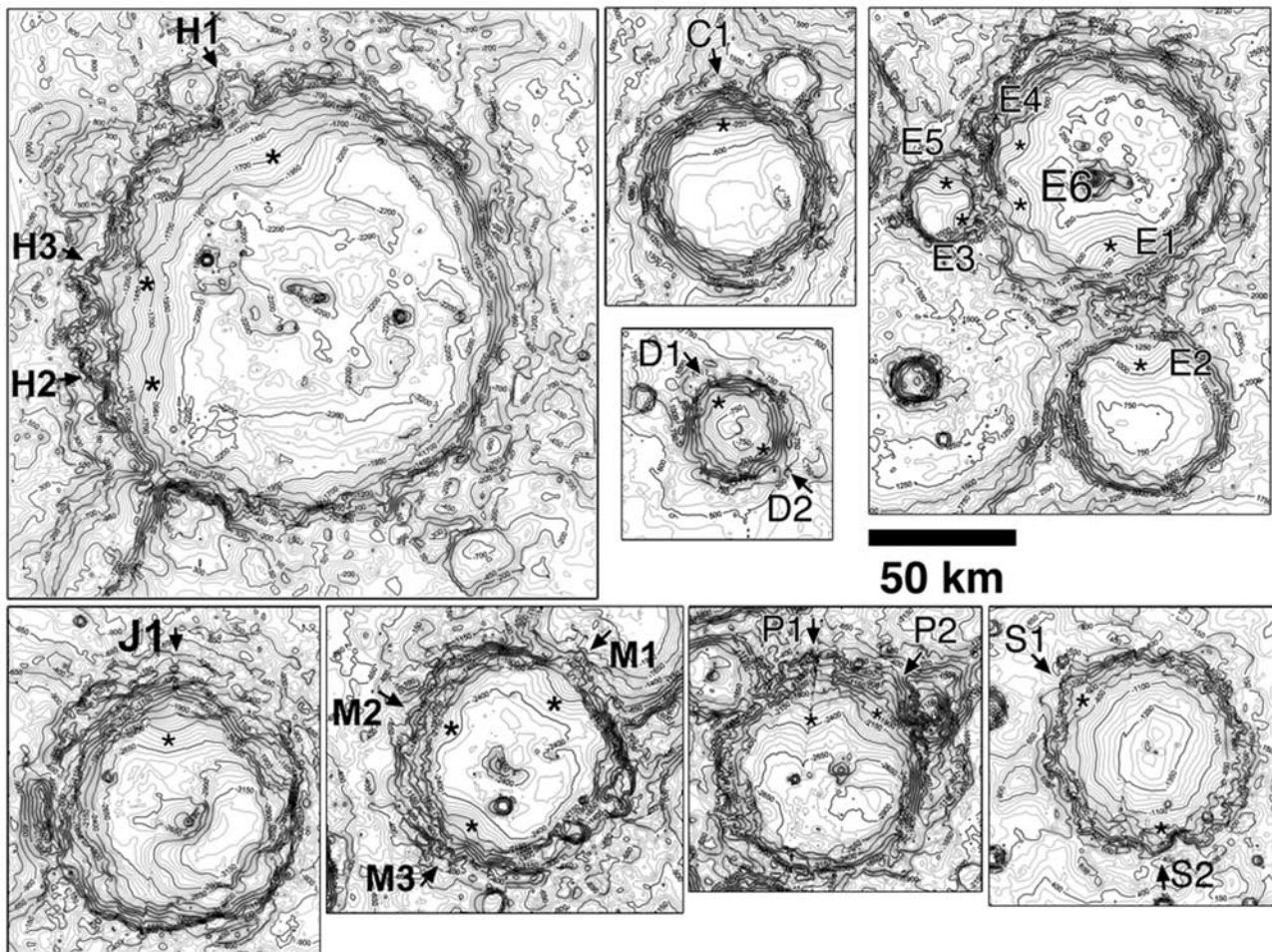


Figure 9



**Figure 10.** The fans (white arrows point to their termini) of 90-km-diameter crater G (centered 27.59°S, 276.74°W) are similar to those of Bakhuisen except that they have well-defined downslope ridge and trough textures. A fan (located at D) at the base of the south rim of crater G might be a delta.

**Figure 9.** In contrast to large fans, such as those in Holden (Figures 7 and 8), the fans of 157-km-diameter Bakhuisen (centered 23.2°S, 344.2°W) have no hectometer-scale texture, tend to have very low or no distal lobe bounding scarp (black arrows), have noticeably concave longitudinal profiles with gradients of  $<0.4^\circ$  to  $1.5^\circ$  (there are 200 m of relief between the arrows in Figure 9d), and have relatively large, relatively high-order source channels. The source channels incise preexisting smooth and presumably sediment-filled basins as they travel from their catchments to the fans. However, expression of channels on the fans themselves is either, at best, muted or nonexistent, although isolated patches of older material surrounded by a fan will be channeled. (a) MOLA-derived DEM of Bakhuisen with THEMIS images superposed to provide context. Right outline shows the location of Figure 9b, and left outline shows location of Figure 9c. Nested left box shows the location of Figure 9d. (b) Portion of THEMIS daytime IR image I01573002 and (c) portion of THEMIS daytime IR image I07927003, both 32 km wide. (d) Portion of THEMIS VIS image V07927004, 17.4 km wide. North is up. Illumination is from the west.



**Figure 11.** MOLA-derived topographic maps (50 m contour intervals) showing the locations, along with Figures 4d, 5b, and 6d, of the 31 Martian alluvial fans used for morphometric statistics. See Table 2 for individual fan locations and measurements.

peak (Figure 5). Seven of the fans in this crater are large and discrete enough in MOLA derived digital terrain models (DTMs) to be used in our fan statistics (Table 2).

[11] High-quality MOC NA images ( $\sim 5$  m/pixel) traverse portions of the two large fans in 84-km-diameter crater K (centered  $22.1^{\circ}\text{S}$ ,  $286.8^{\circ}\text{W}$ ), allowing observations of fan surface texture and erosion-accentuated bedding at hectometer scale (Figure 6). These images show differentially eroded fan deposits where erosion-resistant center beds are exposed after finer side-bed material has been removed, presumably by the wind, resulting in ridge-dominated topographic inversion reminiscent of the bedding expression of the delta deposit in Eberswalde [Malin and Edgett, 2003; Moore et al., 2003]. Individual ridges are typically 100 to 200 m wide, with the widest approaching  $\sim 1$  km, while others are only a few tens of meters across. The ridges are overwhelmingly flat-topped and have locally low relief ( $<10$  m). The broader ridges display longitudinal lineations, which in some cases resolve to be even smaller, flat-topped, and very low ridges. Ridges are often stacked on one another, exhibiting crosscutting and superposition. Narrow nested sinuous ridge sets we interpret to be scroll bars, and radiations of narrow branching sinuous ridges interpreted to be finely digitate distributaries are observed mid-fan of fan

K2 (Figure 6a). Near the periphery (toe) of this same fan are seen broad, sinuous-sided ridges we interpret to be terminal gravel sheets (Figure 6b). The apparent presence of scroll bar deposits and branching sinuous channel deposits and the absence of coarse-particle armored flow lobes with convex scarp relief, in addition to the fan's great length (35 km), are all supportive of the hypothesis that this fan was fluvial rather than debris fed [e.g., Blair and McPherson, 1994].

[12] The fans of 145-km-diameter Holden crater (centered  $26.3^{\circ}\text{S}$ ,  $33.9^{\circ}\text{W}$ ) are large, numerous (at least 16), are laterally integrated into a bajada complex, and have interacted with an apparent fluvial-lacustrine system fed by Uzboi Valles that entered on the southwest side of Holden and exited through a breach in the eastern wall (Figure 7). The fans of the western and northern rim are especially large. The fans' morphology suggests an extended period of depositional activity that started prior to and extended through the time period of the throughflowing fluvial-lacustrine system. All but a few fans receiving late stage, apparently post-Uzboi deposition (e.g., Fan H1; see Figure 11 for location) have noticeably trimmed toes, presumably by the through-flowing fluvial system. The formation of prominent fan head entrenchment on the Holden fans may be the response to removal of material

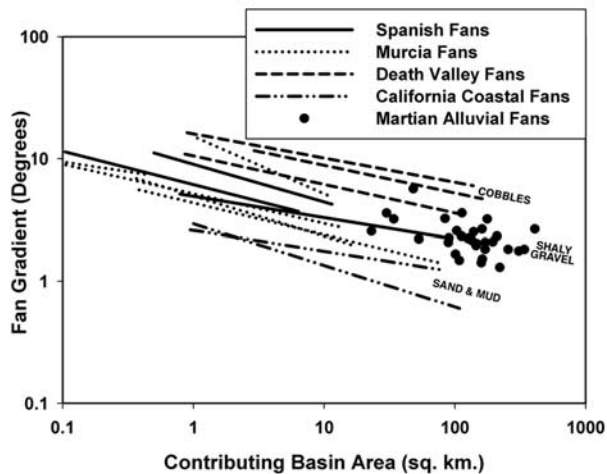


**Figure 12.** Martian alluvial fan data are superimposed on published terrestrial relationships, showing that as with terrestrial fans, larger contributing areas are associated with smaller fan gradients. For a given drainage area, the Martian fans are generally gentler than terrestrial fans in active tectonic settings (Death Valley Region), which generally are composed of coarse gravel and cobble and are steeper than California Coast Range fans that are composed of much finer sediment [Harvey, 1997]. (Terrestrial data in Figures 12, 13, and 14 are from Harvey [1997].)

from their lowest peripheries [e.g., Mack and Leeder, 1998]. Several fanheads near the entrance of Uzboi Vallis into Holden are dissected by flat-floored channels, with a main fanhead trench that branches into a network of distributary channels (Figure 8). As these fans form on inward-facing crater rim walls, they inevitably nearly all coalesce to form uneven bajadas. Locally, highly dissected terrain (outlined in Figure 7) at the foot of the crater wall

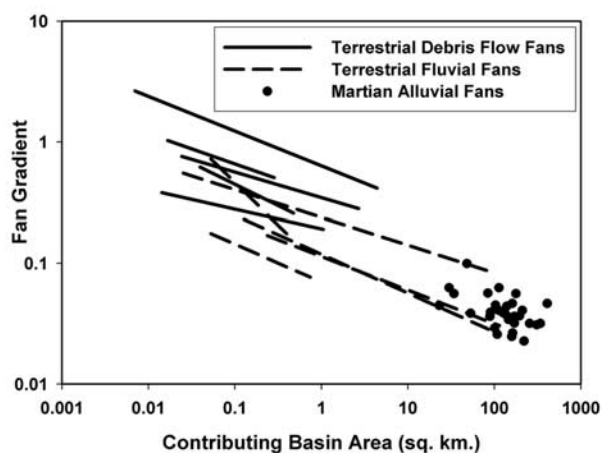


**Figure 13.** Fan gradient versus contributing basin area. The Martian fans, being large and relatively gentle, fall within the terrestrial fluvial portion of the plot. Terrestrial debris flow fans tend to be steeper than fluvial fans for the same contributing area, and most large alluvial fans are fluvial.

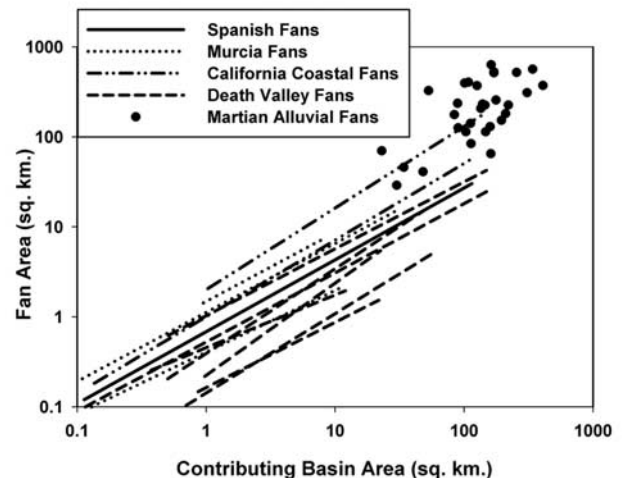


**Figure 14.** Fan area versus contributing basin area. Martian fans tend to be larger relative to their contributing area than terrestrial fans. One reason for this may be the strong limitation on contributing basin size imposed by the crater rims. The lack of tectonic deformation in the case of Martian craters may also have permitted fans to grow to relatively large size.

appears to define an early stage of fan deposition, which was subsequently eroded during later fan emplacement. The fans of the south rim are more isolated and small relative to those in the west and north. These southern fans also have trimmed toes. There appear to be no fan deposits along the east rim. The upper components of layered deposits (seen in MOC NA images [Malin and Edgett, 2000a]) exposed by “Uzboi” erosion just inside and paralleling the south rim of Holden may, in part, be composed of in-place alluvial fan deposits as these layers appear, in some cases, emerging from the scarps of the toe-trimmed fans.

[13] The Martian alluvial fans described thus far have generally been similar to each other in overall morphology. They typically have roughly constant gradients of  $\sim 2^\circ$ , tended to be tear or wedge shape in plan view, in which the length and greatest width have been around a factor of two of each other, and have textures usually dominated by downslope ridges. In contrast, the fans of 157-km-diameter Bakhuisen (centered  $23.2^\circ\text{S}$ ,  $344.2^\circ\text{W}$ ) have no hectometer-scale texture, tend to have very low or no distal lobe bounding scarp, have noticeably concave longitudinal profiles with gradients of  $<0.4^\circ$  to  $1.5^\circ$ , and have relatively large, relatively high-order source channels (Figure 9). The source channels incise preexisting smooth and presumably sediment-filled basins as they travel from their catchments to the fans. However, expression of channels on the fans is either, at best muted, or nonexistent, although isolated patches of older material surrounded by a fan will be channeled. These fans may be transitional between the class of fans such as are seen in craters A, L and Holden, and the alluvial or fluvial delta reported by Malin and Edgett [2003] and Moore et al. [2003]. The fans of 90-km-diameter crater G (centered  $27.59^\circ\text{S}$ ,  $276.74^\circ\text{W}$ ) are similar to those of Bakhuisen except that they have well-defined downslope ridge and

**Table 3a.** Morphometric Properties of Alluvial Fans in Basin and Range Province, Nevada and California<sup>a</sup>

1:24,000 Quadrangle Name	Source Basin Mountain Range	Catchment Relief, km	Catchment Gradient, km/km	Fan Gradient, km/km	Fan Concavity, km <sup>-1</sup>	Fan Length, km
Amboy	Clipper	0.25	0.246	0.0674	— <sup>b</sup>	14.6
Amboy	Piute	0.10	0.197	0.0262	—	15.0
Amboy	Providence, E <sup>c</sup>	0.60	0.215	0.0538	—	12.8
Amboy	Providence, W	0.55	0.197	0.0463	0.0930	25.5
Bishop	Inyo, W	0.30	0.148	0.0984	—	14.0
Bishop	Sierra, NE	2.00	0.328	0.0716	0.2021	22.0
Blythe	McCoy, W	0.55	0.271	0.0112	0.2147	22.0
Blythe	Big Maria, W	0.30	0.197	0.0134	—	22.0
Blythe	Planosa, W	0.20	0.197	0.0123	0.0358	32.0
Borrego Valley	Santa Rosa, W	1.22	0.511	0.0917	—	7.3
Borrego Valley	Santa Rosa, E	1.10	0.333	0.0557	0.1948	23.5
Coalinga	Joaquin, E	0.85	0.093	0.0098	0.1879	36.0
Cuddleback Lake	Gravel Hills, SW	0.10	0.056	0.0256	0.1636	21.5
Cuttleback Lake	Black Hills, W	0.10	0.197	0.0325	0.1369	23.0
Darwin Hills	Argus, E	1.50	0.246	0.0422	0.0000	14.0
Darwin Hills	Argus, W	0.50	0.281	0.0926	0.8841	8.5
Darwin Hills	Panamint, W	1.00	0.112	0.0937	0.2812	10.5
Death Valley Junction	Panamint, E	1.00	0.207	0.0802	0.1053	13.5
Death Valley Junction	Nopah, W	0.60	0.251	0.0497	0.4856	9.3
Death Valley Junction	Nopah, E	0.70	0.276	0.0447	0.7211	11.0
Delano	Temblor, E	0.35	0.119	0.0128	0.1461	46.2
Eagle Mtns.	Granite, W	0.50	0.219	0.0300	0.1825	29.5
Eagle Mtns.	Chuckwalla, W	0.35	0.276	0.0248	0.1017	51.5
Lancaster	Teckopi, SE	0.55	0.135	0.0295	0.1321	28.0
Last Chance	Amargosa, NW	0.30	0.098	0.0962	0.3219	9.0
Mesquite Lake	Clark	0.40	0.079	0.0570	0.2266	19.0
Mount Whitney	Sierra Nevada, E	1.95	0.243	0.0621	0.0083	22.2
Needles	Sacramento, SW	0.10	0.028	0.0149	0.1082	29.0
Needles	Sacramento, NE	0.30	0.197	0.0215	0.1213	32.0
Newberry Springs	Cody, NE	0.25	0.164	0.0583	—	13.5
Newberry Springs	Bristol, SW	0.20	0.098	0.0428	—	11.5
Newberry Springs	Roduca, N	0.25	0.062	0.0525	0.1453	15.0
Owlshead Mountains	Avawatz, ME	1.10	0.155	0.0197	0.3555	30.0
Owlshead Mountains	Nopah, W	0.85	0.239	0.0591	0.3750	10.0
Ridge Crest	Slate, W	0.50	0.141	0.0656	—	9.0
Ridge Crest	Slate, E	0.75	0.268	0.0844	—	3.5
Saline Valley	Nelson, NW	1.35	0.332	0.0787	0.2784	10.0
Saline Valley	Cottonwood, NE	1.80	0.169	0.1148	0.5624	6.0
Saline Valley	Tin, NE	1.20	0.197	0.1083	0.0895	10.0
Salton Sea	Chocolate, SW	0.40	0.157	0.0219	0.1312	18.0
Sheep Hole Mountain	Sheep Hole, NE	0.50	0.328	0.0432	0.1723	20.5
Sheep Hole Mountain	Unnamed	0.35	0.115	0.0422	—	14.0
Sheep Hole Mountain	Old Woman, SE	0.20	0.131	0.0371	0.0882	26.5
Soda Mountains	Soda, SW	0.32	0.485	0.0999	—	6.7
Soda Mountains	Soda, E	0.30	0.148	0.0591	—	10.0
Soda Mountains	Unnamed, S	0.24	0.236	0.0465	—	11.0
Las Vegas	Spring, SW	1.30	0.205	0.0545	0.0844	41.5
Las Vegas	Spring, N	0.80	0.262	0.0769	0.0608	32.0
Beatty	Amargosa, SW	0.50	0.179	0.0747	0.1829	14.5
Boulder City	White Hills, W	0.15	0.084	0.0382	0.0662	33.5
Cactus Flat	Cactus, SW	0.25	0.164	0.0466	0.1234	19.0
Cactus Flat	Kawitch, SW	0.25	0.082	0.0193	0.0921	52.0
Cactus Flat	Kawitch, NE	0.20	0.123	0.0316	—	21.8
Cactus Flat	Reveille, W	0.15	0.118	0.0437	—	13.5
Cactus Flat	Reveille, E	0.35	0.276	0.0815	—	14.5

<sup>a</sup>Alluvial fans in the basin province of Nevada and California were measured from 1:24,000 topographic maps.

<sup>b</sup>No data available.

<sup>c</sup>Compass location of fan relative to mountain range.

trough textures (Figure 10). A fan (D in Figure 10) emerging from the south rim of crater G might correctly be classified as a delta.

### 2.3. Fan Morphometrics and Comparison With Terrestrial Fans

[14] The excellent preservation of the fans discussed here permits measurement of many of the morphometric properties that are commonly used to analyze terrestrial alluvial

fans. Terrestrial fans are typically characterized by the relationship between fan gradient or fan area and such factors as catchment area, basin relief, and sediment grain size (e.g., reviews by *Blair and McPherson* [1994] and *Harvey* [1997]). In tectonically active areas on Earth (e.g., in the Basin and Range Province) these relationships are complicated by tilting and faulting of the fan and catchment [e.g., *Denny*, 1965; *Bull*, 1964], a situation apparently not a factor for the Martian fans.



**Table 3b.** Morphometric Properties of Terrestrial Low-Relief Alluvial Ramps<sup>a</sup>

1:250,000 Topographic Quadrangle	Catchment Relief, km	Catchment Gradient, km/km	Fan Gradient, km/km	Fan Concavity, km <sup>-1</sup>	Fan Length, km
Millet	0.81	0.110	0.0414	0.1983	8.5
Millet	0.86	0.198	0.0150	0.1046	3.6
Millet	0.66	0.123	0.0067	0.3637	8.0
Needles	0.33	0.128	0.0235	0.2156	5.4
Phoenix	0.52	0.107	0.0129	0.3601	7.2
Phoenix	0.26	0.095	0.0197	0.0305	6.8
Pueblo	1.15	0.138	0.0385	0.3711	6.3
Pueblo	0.96	0.108	0.0221	0.2144	7.2
Tucson	0.57	0.261	0.0040	0.1628	18.1
Tucson	0.96	0.125	0.0302	0.0766	15.6
Tucson	0.72	0.149	0.0431	0.0379	8.5
Ajo	0.42	0.111	0.0083	0.1081	9.9
Ajo	0.22	0.082	0.0052	0.3789	9.3
Ajo	0.38	0.256	0.0141	0.4156	5.0
Charlottesville	0.52	0.143	0.0232	0.3756	5.2
Charlottesville	0.67	0.054	0.0124	0.2297	12.2
Charlottesville	0.34	0.097	0.0177	0.9292	5.0
Fresno	3.28	0.039	0.0018	0.0561	74.7
Fresno	2.62	0.043	0.0019	0.0378	71.0
Cheyenne	0.54	0.020	0.0055	0.0144	83.4
Cody	1.70	0.031	0.0060	0.0149	81.2
Craig	0.87	0.060	0.0071	0.1483	18.1
Delta	0.23	0.032	0.0299	0.1180	7.9
Denver	1.72	0.034	0.0042	0.0552	46.9
Elko	1.15	0.130	0.0100	1.2752	5.9
Elko	1.58	0.234	0.0126	0.0167	3.8
Ely	1.47	0.220	0.0235	0.6384	8.4
Ely	0.79	0.174	0.0176	0.3346	9.9
Greeley	2.39	0.056	0.0025	0.0254	96.1
Lovelock	0.99	0.190	0.0322	0.3331	5.5
Lovelock	1.12	0.183	0.0274	0.3103	8.9
Mariposa	1.73	0.153	0.0257	0.0907	11.7

<sup>a</sup>The low-relief alluvial ramp data were extracted from 3 arc-second DEMs of 1:250,000 topographic maps.

### 2.3.1. Measurements

[15] Although sedimentary characteristics of the Martian fans are uncertain, the gross morphometry of the fans can be readily measured from a combination of available THEMIS VIS and IR images and MOLA topography. For each of the craters containing fans we prepared MOLA topographic maps from individual orbit tracks in Precision Experiment Data Record (PEDR) data releases converted into a Digital Elevation Model (DEM) in the commercial program SURFER by natural neighbor interpolation to a resolution of 0.5 km square pixels. We utilized the original MOLA track data in order to examine individual MOLA profiles and to assess whether the density of data was sufficient to define the fan and headwater basin morphology. In an initial exercise we defined the catchment basin periphery and fan outline for eight fans from THEMIS IR images and compared measurements of fan and catchment area measured on contour maps produced in SURFER from the DEM data. The catchment basin was measured on contour maps as delineated by its drainage divide. The lateral boundaries of the fan were generally well marked by aligned, abrupt contour planform bends at edge of the convex fan form. The base of the fan was defined as the location of the abrupt decrease of topographic gradient. The measurements agreed within 10 percent. The close agreement permitted us to measure areas for fans from contour maps for which THEMIS VIS or IR coverage was missing or incomplete.

[16] An important location on an alluvial fan is the upper end of the fan, or the apex, which separates the fan proper from the contributing drainage basin. We defined the fan apex as the location at which the planimetric form of contours changed downstream from concave (convergent flow) to convex (divergent flow). The apex as so defined is not necessarily the headward terminus of alluvial deposition, because continuing sediment aggradation commonly buries the lower portion of the main stem contributing basin channel.

[17] Relief characteristics of the fan and contributing basin were measured by digitizing a topographic profile along the line of steepest descent from the divide of the contributing basin through the apex to the base, or terminus, of the fan. Within the contributing basin the profile started at a point on the drainage divide opposite the apex and at approximately the mean elevation of the terminal drainage divide, avoiding extreme high or low points along the divide. The downstream distance and elevation along this profile were measured at four locations: the contributing basin divide, the fan apex, the midpoint of the fan, and the fan terminus.

[18] Two data sets were utilized for comparison with 31 Martian fans (Figures 4d, 5b, 6d, and 11). For comparison with published data on terrestrial alluvial fans (Figures 12–14) we measured the relief characteristics as well as fan and contributing basin areas. A separate collection of data on relief characteristics of terrestrial fans and alluvial surfaces as well as Martian crater floors

**Table 3c.** Morphometric Properties of Noachian Crater Floors<sup>a</sup>

West Longitude, deg	Latitude, deg	Crater Diameter km	Catchment Relief, km	Catchment Gradient, km/km	Fan Gradient, km/km	Fan Concavity, km <sup>-1</sup>	Fan Length, km
271.4	-0.7	38.5	2.06	0.310	0.0086	0.2109	12.8
271.4	-0.7	38.5	1.42	0.167	0.0118	0.4257	10.6
266.4	-5.0	75.5	2.85	0.153	0.0043	0.1536	25.9
266.4	-5.0	75.5	2.07	0.174	0.0105	—	5.7
272.3	-6.1	20.8	0.72	0.232	0.0162	0.4356	7.0
272.3	-6.1	20.8	0.74	0.270	0.0365	1.6094	1.3
274.1	-4.6	23.1	0.82	0.128	0.0131	0.1898	11.8
274.1	-4.6	23.1	0.51	0.342	0.0384	—	0.9
274.0	-3.9	19.2	0.57	0.307	0.0120	0.1444	4.2
274.0	-3.9	19.2	0.63	0.157	0.0223	—	1.2
271.7	-3.3	38.9	0.32	0.268	0.0128	0.0314	20.7
271.7	-3.3	38.9	0.31	0.148	0.0067	0.0374	14.9
272.0	-4.9	27.9	0.21	0.136	0.0064	0.1267	11.3
272.0	-4.9	27.9	0.36	0.101	0.0079	0.0339	6.1
272.8	-3.3	54.2	0.87	0.284	0.0276	0.0828	15.2
272.8	-3.3	54.2	1.38	0.130	0.0132	-0.0532	15.3
273.3	-5.7	31.4	0.89	0.207	0.0106	0.0151	11.8
273.3	-5.7	31.4	0.99	0.292	0.0385	0.5059	3.0
2.9	-19.9	80.6	0.66	0.051	0.0050	0.0948	27.5
2.9	-19.9	80.6	0.89	0.211	0.0067	0.0724	26.1
4.1	-21.2	75.0	0.43	0.099	0.0075	0.0900	29.1
4.1	-21.2	75.0	0.25	0.037	0.0083	0.1114	23.9
3.4	-19.2	33.6	0.89	0.193	0.0111	0.0589	13.7
3.4	-19.2	33.6	1.21	0.199	0.0092	0.2453	9.2
16.3	-19.4	19.0	0.36	0.119	0.0083	0.3300	5.2
16.3	-19.4	19.0	0.52	0.188	0.0098	0.4076	7.9
358.6	-29.4	70.1	1.78	0.242	0.0108	0.0931	19.0
358.6	-29.4	70.1	1.63	0.130	0.0204	0.1613	5.8
14.5	-18.8	48.3	1.15	0.268	0.0079	0.1061	20.2
14.5	-18.8	48.3	1.14	0.311	0.0213	0.0772	12.8
12.0	-18.4	68.3	1.49	0.222	0.0119	0.1283	24.7
12.0	-18.4	68.3	1.62	0.177	0.0166	-0.1161	11.9
9.1	-21.2	79.8	1.26	0.258	0.0069	0.1072	22.9
9.1	-21.2	79.8	1.34	0.096	0.0060	0.0493	28.1
9.2	-18.7	55.1	1.28	0.209	0.0156	0.1554	15.3
9.2	-18.7	55.1	1.49	0.232	0.0148	0.1193	17.1
22.8	-19.2	64.7	1.94	0.167	0.0107	0.1439	14.0
22.8	-19.2	64.7	1.84	0.099	0.0116	0.2487	14.0
24.3	-18.3	48.1	1.55	0.196	0.0104	0.3383	15.3
24.3	-18.3	48.1	1.73	0.236	0.0127	0.1430	11.3
24.6	-19.7	16.2	0.20	0.111	0.0083	0.1345	4.3
24.6	-19.7	16.2	0.18	0.120	0.0128	0.2021	8.6
17.6	-24.4	54.1	1.39	0.165	0.0128	0.1313	17.6
17.6	-24.4	54.1	1.75	0.191	0.0098	0.1119	18.3
18.0	-23.2	35.4	1.05	0.216	0.0213	0.5307	4.6
18.0	-23.2	35.4	1.07	0.141	0.0054	0.1378	16.5
8.0	-24.1	16.9	0.36	0.129	0.0135	0.4494	4.6
8.0	-24.1	16.9	0.35	0.165	0.0100	0.7040	5.5
8.4	-25.1	19.3	0.41	0.166	0.0135	0.1977	6.1
8.4	-25.1	19.3	0.54	0.195	0.0138	0.1572	7.6
9.1	-23.1	29.4	0.92	0.231	0.0114	0.4100	9.2
9.1	-23.1	29.4	0.95	0.183	0.0120	0.3584	7.9
22.9	-24.6	85.2	2.49	0.163	0.0070	0.1942	15.6
22.9	-24.6	85.2	2.03	0.125	0.0110	0.2785	13.2
22.9	-24.6	87.1	2.46	0.192	0.0091	0.1573	11.7
22.9	-24.6	87.1	1.87	0.165	0.0140	0.5837	8.9

<sup>a</sup>The Martian crater data were collected from inward-sloping crater floor surfaces on opposite sides of each of 26 sampled impact craters, which are identified by longitude, latitude, and crater diameter. These measurements were made from individual MOLA PEDR profiles.

was compiled by *Howard and Craddock* [2000] and *Craddock and Howard* [2002] (Tables 3a, 3b, and 3c) in order to quantify fan concavity, which has not generally been measured on terrestrial fans. Because the bajada-like Noachian crater floors had apparent sediment sources from nearly uniformly distributed small gullies on crater walls, unique fans and contributing areas could not be distinguished. Similar relief data were collected for terrestrial

basin deposits. These additional data sets are described below:

### 2.3.1.1. Noachian Degraded Crater Floors

[19] *Howard and Craddock* [2000] and *Craddock and Howard* [2002] noted that the floors of strongly degraded Noachian craters that appeared to be flat-floored in Viking images actually sloped gently from the base of the interior crater rim to the crater center. They interpreted these to be

**Table 4.** Regressions Between Martian Fan Properties<sup>a</sup>

Dependent Variable	Independent Variable	Multiplicative Constant	Exponent	R <sup>2</sup>
Fan size <sup>b</sup>	Contributing basin size	4.26	0.79	0.42
Fan size	Contributing basin gradient	10.5	-1.32	0.31
Fan gradient <sup>c</sup>	Contributing basin gradient	0.125	0.52	0.33
Fan gradient	Contributing basin size	0.117	-0.22	0.23
Fan gradient	Fan size	0.151	-0.25	0.44

<sup>a</sup>Regressions between the logarithms of the variable are expressed as  $Y = mX^n$ , where  $Y$  is the dependent variable,  $X$  is the independent variable,  $m$  is the multiplicative constant, and  $n$  is the exponent. Only statistically significant relationships are included.

<sup>b</sup>Fan and contributing basin size are in km<sup>2</sup>.

<sup>c</sup>Gradients are expressed as slope tangent.

depositional bajadas of sediment eroded from the rims. Measurements were made of fans on the opposite walls of 28 representative craters having basin floor gradients ranging from 0.25° to 2.2°, averaging 0.74°. These are designated as Martian degraded crater floors in figure captions.

### 2.3.1.2. Terrestrial Alluvial Fans

[20] Profile measurements were made through 55 terrestrial alluvial fans in tectonically active settings in the Basin and Range province of southern Nevada and California from 1:24,000 topographic maps. Fan lengths varied from 6 to 45 km, with gradients from 0.56° to 6.6°, averaging 3.0°. The relatively steep gradients probably result from both high basin relief and the coarse texture of the supplied sediment.

### 2.3.1.3. Terrestrial Low-Relief Alluvial Surfaces

[21] Fans and depositional plains were also measured in a variety of relatively stable tectonic settings. Locations varied from southern Arizona and New Mexico to northern Nevada, the Rocky Mountain region of Colorado and Wyoming and fans in the Shenandoah Valley of Virginia. Basin length varied from 3.6 to 96 km, and gradients ranges from 0.1° to 2.5°, averaging 1.0°. Measurements were made from 1:250,000 digital DEMs. These are designated as terrestrial alluvial surfaces in figure captions.

[22] Relief characteristics that were measured for each of these data sets include (1) average gradient from apex to fan base, (2) contributing basin relief, (3) contributing basin average gradient from divide to apex, and (4) fan concavity. Fan concavity,  $B$ , was measured by fitting a negative exponential function to the fan profile from apex to base, with the governing equation being

$$z = z_{\infty} + (z_a - z_{\infty}) \exp[-B(x - x_a)], \quad (1)$$

where  $z$  is the local fan elevation,  $z_a$  is the elevation at the fan apex,  $z_{\infty}$  is the fan elevation at the hypothetical downstream base level, and  $x$  is the distance downstream from the apex at  $x_a$ . The concavity,  $B$ , can be expressed as a function of the first and second derivatives of  $z$ :

$$B = \frac{-d^2z/dx^2}{dz/dx}. \quad (2)$$

The derivatives were estimated from measurements of elevation and downstream distance made at the fan apex, midpoint, and base, and these were substituted into (2) to estimate  $B$ .

### 2.3.2. Results

[23] Regressions between measured morphometric parameters for the Martian fans indicate statistically significant (at

the 5% level of significance) positive log-log relationships between fan gradient and contributing basin gradient and between fan size and contributing basin size (Table 4). Statistically negative log-log relationships occur between fan gradient and fan size, fan gradient and contributing basin size, and fan size and contributing basin gradient. No significant relationships were found between fan size or fan gradient and contributing basin relief.

[24] In general both the Martian alluvial fans and the Noachian crater floors have morphometric characteristics that fall within the range of terrestrial alluvial fans or basins. In the terrestrial literature it is common to correlate fan gradient with contributing basin area. In Figure 12 the Martian alluvial fan data are superimposed on published terrestrial relationships, showing that, as with terrestrial fans, larger contributing areas are associated with smaller fan gradients. For a given drainage area, the Martian fans are generally gentler than terrestrial fans in active tectonic

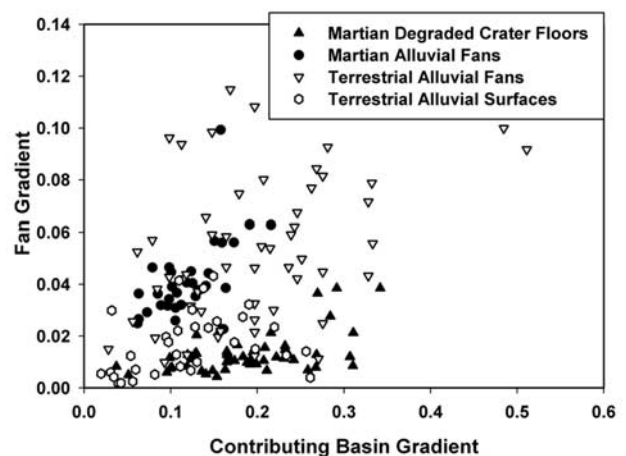


**Figure 15.** Terrestrial alluvial fans and alluvial surfaces as well as Martian alluvial fans and Noachian degraded crater floors show a positive correlation between the depositional basin gradient and the contributing basin gradient. The Martian alluvial fans generally fall on the same trend as the terrestrial alluvial fans, whereas the gentler Noachian crater floor ramps are similar in gradient to the low-relief terrestrial alluvial surfaces. (Figures 15–17 data are from our present measurements (Tables 3a, 3b, and 3c) and Craddock and Howard [2002]. Note that “gradient” in these three figures has the traditional slope tangent definition so that our measurements could be compared with the published terrestrial data.)

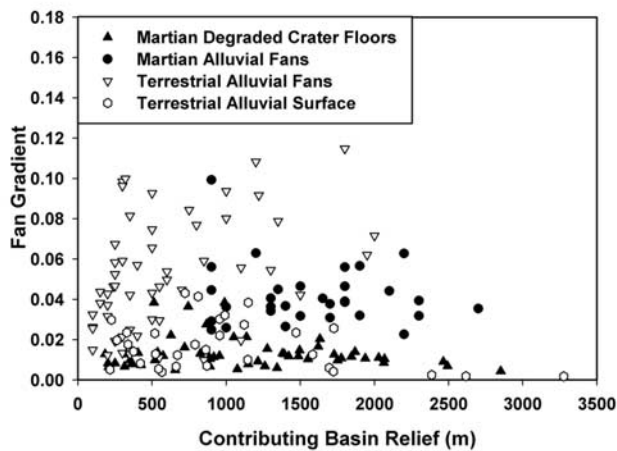


**Figure 16.** In both terrestrial and Martian alluvial deposits there is little correlation between contributing basin relief and depositional basin gradient. However, for a given fan gradient, Martian alluvial fans generally have greater source basin relief than terrestrial fans in active tectonic settings. This suggests that the terrestrial source basins either yield coarser debris or have higher sediment concentrations than their Martian counterparts.

settings (Death Valley Region) which generally are composed of coarse gravel and cobbles and are steeper than California Coast Range fans that are composed of much finer sediment such as sand and silt (e.g., *Harvey* [1997]; see references in his Figure 12.7 caption).

[25] The relationship between fan gradient and contributing area has also been used to distinguish between fans formed by fluvial deposition versus mudflows. Terrestrial debris flow fans tend to be steeper than fluvial fans for the same contributing area, and most large alluvial fans are fluvial (Figure 13). The Martian fans, being large and relatively gentle, fall within the terrestrial fluvial portion of the plot (Figure 13).

[26] Another common comparison in the terrestrial literature is to compare alluvial fan size to that of the contributing basin (Figure 14). Martian fans tend to be larger relative to their contributing area than sampled terrestrial fans. One reason for this may be the strong limitation on contributing basin size imposed by the crater rims. The lack of tectonic deformation in the case of Martian craters may also have permitted fans to grow to relatively large size.

[27] Terrestrial alluvial fans and alluvial surfaces as well as Martian alluvial fans and Noachian degraded crater floors show a positive correlation between the depositional basin gradient and the contributing basin gradient (Figure 15, Table 4). The Martian alluvial fans generally fall on the same trend as the terrestrial alluvial fans, whereas the gentler Noachian crater floors are similar in gradient to the low-relief terrestrial alluvial surfaces.

[28] In both terrestrial and Martian alluvial deposits there is little correlation between contributing basin relief and depositional basin gradient (Figure 16). However, for a given fan gradient, Martian alluvial fans generally have greater source basin relief than terrestrial fans in active tectonic settings. This suggests that the terrestrial source

basins either yield coarser debris or have higher sediment concentrations than their Martian counterparts.

[29] The Martian alluvial fans have relatively low profile concavity (Figure 17), although there is a tendency for concavity to be greater for steeper fans. The estimated concavity,  $B$ , of the Martian fans (average  $0.070 \text{ km}^{-1}$ ) is significantly lower than that of the Noachian degraded crater floors (0.224), terrestrial alluvial fans (0.207) and terrestrial low-relief alluvial surfaces (0.251). The mean concavities of the latter three data sets are statistically indistinguishable.

## 2.4. Age

[30] Determining the age of the fans under investigation directly from crater statistics is difficult, largely because of their small size. All the fans, regardless of location, have numerous small craters on their surfaces where seen in  $\sim 17 \text{ m/pixel}$  THEMIS VIS or  $2\text{--}5 \text{ m/pixel}$  MOC NA images (e.g., Figure 6), indicating that they are not “modern,” unlike the small gully and debris aprons of the mid latitudes first reported by *Malin and Edgett* [2000b], which are uncratered, or the small uncratered fans recently reported by *Williams et al.* [2004]. All fan-containing craters are found exclusively within Noachian terrains in the global mapping of *Greeley and Guest* [1987] and *Scott and Tanaka* [1986].

[31] Using available (as of July 2004) THEMIS daytime IR coverage of these fans, and assuming that the fans were essentially contemporaneous (which is, itself not been strictly demonstrated), the total crater count area of fans is  $14,128 \text{ km}^2$ , on which there are 31 craters  $\geq 1 \text{ km}$  in diameter. Applying the square root of two uncertainly to this statistic yields a density probability of  $31 \pm 5.57$ , or normalized to a standard crater counting area gives a value of  $2194.18 \pm 394$  craters  $\geq 1 \text{ km}$  per  $10^6 \text{ km}^2$ . Using this

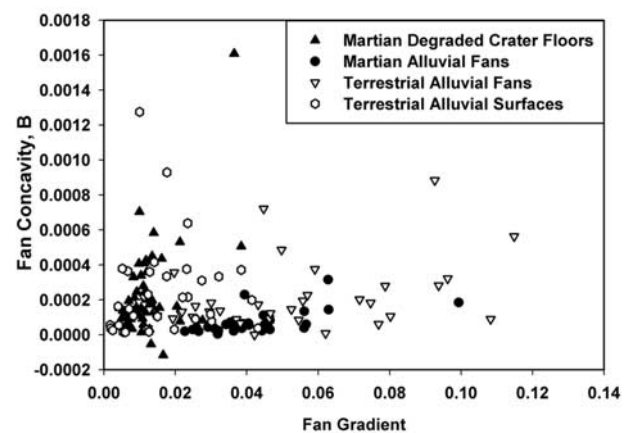


**Figure 17.** The Martian alluvial fans have relatively low profile concavity, although there is a tendency for concavity to be greater for steeper fans. Concavity is defined by fitting fan profiles to equation (1). This low concavity is similar to the concavity of terrestrial alluvial fans in active tectonic settings. By contrast, on the average, Noachian degraded crater floor ramps and low-relief terrestrial alluvial surfaces exhibit higher concavities.

value and its uncertainty with the new crater density-to-age relationship reported by *Hartmann and Neukum* [2001], the nominal age of the fans is 3.35 GA (mid Hesperian), with an uncertainty range from 3.7 GA (Noachian-Hesperian boundary) to 1.6–1.1 GA (mid Amazonian). The age of the fans derived from crater statistics may be a minimal value, as the fans may have had protective aeolian-transported mantles for long periods after they were formed, preventing impacts from marring the surfaces we see exposed today, as was apparently the case with a delta-shaped fluvial deposit located in a small basin just north of Holden [*Moore et al.*, 2003].

[32] The fans, at least in the southern Margaritifer Sinus region (MC-19), are probably not older than late Noachian, as they rest on a late Noachian surface [*Grant*, 1987, 2000]. More constraining is the observation that many of the fans in Holden crater are cut by fluvial erosion associated with Uzboi Vallis, which *Grant* [1987, 2000] dates at very latest Noachian. If the other fans of this study are contemporaries of the Holden fans, then the epoch of these alluvial fans is approximately the Noachian-Hesperian boundary, a time when there may have been an increase in fluvial activity precipitated by a climate optimum [*Howard and Moore*, 2004b].

### 3. Discussion

#### 3.1. Fan Hydraulics and Sedimentology

[33] Terrestrial alluvial fans form from sediments ranging in dominant grain size from mud to coarse gravel and by flows ranging from debris flows to normal fluvial transport, both as channelized and as sheet flows. Sediment size and flow type affect both the fan morphometry as well as surface features. In previous discussion we compared the Martian fan morphometry to their terrestrial counterparts. Inferences about flow processes and dominant grain size are hindered by postdepositional degradation of the Martian fan surfaces, lack of direct information on sediment grain size, and the lower gravity of Martian fans. The gravitational effects are particularly difficult to assess. Gravel bed streams on Earth typically have gradients that are close to the threshold of motion for the dominant bed grain size [e.g., *Howard*, 1980]. Scaling analysis suggests that gravitational effects on fluvial gradients at the threshold of motion should be minor [*Pieri*, 1980; *Komar*, 1980]. However, for equivalent discharge, channel dimensions, and gradient, sediment loads in sand-bed channels should be about 50 percent greater on Mars than on Earth. However, sediment loads supplied from headwater channels may be smaller for equivalent discharges because headwater sediment entrainment depends on flow shear stress [e.g., *Howard*, 1994], which will be lower on Mars. Both of these factors suggest sand-bed fan channels on Mars should have lower gradients than on Earth for equivalent source area relief. Debris flows may require steeper gradients on Mars than Earth in order for shear stresses to be large enough to exceed the yield strength of the debris flow slurry.

[34] For equivalent source basin size, the Martian alluvial fans are closer in gradient to the steep fans of Death Valley dominated by coarse gravels and cobbles than the fine-grained (sand and silt) fans of coastal California (Figure 12).

Given that fine-bed alluvial channels might be gentler on Mars than Earth, we tentatively conclude that the Martian Fans are dominated by gravelly sediment. The low concavity of the Martian fans is also similar to that of the coarse-grained terrestrial alluvial fans of the Basin and Range province (Figure 17). In addition, for a given average gradient in the source basin (Figure 15) and for a given source basin relief (Figure 16), both the Martian fans and Basin and Range fans have steeper gradients than the Noachian degraded craters and terrestrial low-relief alluvial surfaces, which is also consistent with a supply of coarse sediment.

[35] The mode of sediment transport (debris flow versus fluvial) is less certain. Terrestrial debris flow fans are generally both smaller and steeper than fluvial fans (Figure 13). The Martian fans, being both relatively large and low in gradient, fall within the field to terrestrial fluvial fans (Figure 13). On terrestrial alluvial fans with mixed debris flow and fluvial sedimentation, the debris flows commonly are most prevalent on the upper portions of the fan and fluvial on the lower parts [*Hooke*, 1967], presumably because of the greater mobility of fluvial flows. The large size of the Martian fans requires flows capable of traversing tens of kilometers before depositing all sediment. Terrestrial fluvial fans generally display wide, multiple-branching distributaries, which are also apparent on Martian fan K (Figure 6). Taken together, the large size and low gradient of the Martian fans along with bedforms typical of fluvial deposition lead us to favor a fluvial origin for the fans of this study.

#### 3.2. Implications for Paleoclimate

[36] The alluvial fans of this study are not features that could have formed during a single event, such as a catastrophic landslide. Their construction must have taken many years. To gain a sense of the minimum time to emplace a fan, we consider fan A1, which has a surface area of  $\sim 500 \text{ km}^2$ . If we assume, after an inspection of the contour map of this feature (Figure 4d), an arbitrary but reasonable average thickness of this fan as  $\sim 100 \text{ m}$ , we get a volume of  $50 \text{ km}^3$ . For this exercise we use a report of a  $860,000 \text{ m}^3$  deposit emplaced on an alluvial fan in the White Mountains of California during a single event derived from a catchment of  $17 \text{ km}^2$  [*Beaty*, 1970, 1990], ten times smaller than the catchment of fan A1. If we simply scale the White Mountains deposit by the catchment we have a value of  $8.6 \times 10^{-3} \text{ km}^3$ , which, if this amount of material was added every year to the construction of fan A1, it would take  $\sim 5800$  years to form this fan. Of course this ignores the real lapse time between successive deposits necessitated by the need to regenerate a new supply of loose detritus in the catchment susceptible to transportation by flash flood flushing, which in the White Mountains case results in a deposition event of the magnitude reported by *Beaty* [1970, 1990] recurring on average of every  $\sim 320$  years. Recurrence rates for Martian fan deposits is unknown, but the implications of the terrestrial example is that Martian fans probably cannot form in less than a millennia and might reasonably be expected to at least take more on order of 100 millennia. If the precipitation and runoff inducing climate were intermittent, the period of fan growth on Mars could be much longer.

[37] An extended period of fan development is also suggested by the history of fan deposition in Holden crater, where fan development both preceded and followed the time period of flows from Uzboi Valles through the crater. Although a single, geologically short-lived event of complicated history could be proposed to produce such a situation, similar terrestrial scenarios of fan evolution typically require millennia to millions of years.

[38] The feature of the Martian alluvial fans that most distinguishes them from terrestrial counterparts is their geographic restriction, both planet-wide and within craters. Fan-hosting craters have been found only within a narrow latitudinal belt, and only in three widely separated crater clusters within that belt (Figure 1). Within individual craters the fans almost universally originate from erosion of deeply incised alcoves in the crater walls. Most of the craters have alcove incision and fan deposition along at limited sites on the crater walls (e.g., Figures 4, 10, and 11), although a few support fans along half or more of the interior crater wall (e.g., Figure 5). Possible reasons for geographic isolation include climatic factors, variations in crater wall lithology, unique physiography of fan-producing crater walls, and local triggering mechanisms, such as effects of nearby impacts. We discount the latter two mechanisms as realistic causes. Although craters hosting fans are limited to steep, deep craters of late Noachian age, we have no evidence to suggest that such craters are restricted to the three planetary locations that we have found fans. Similarly, within craters the crater walls producing alcoves and fans appear not to be universally associated with particularly steep or high locations on the crater walls, although this may be a factor in fan location in Crater A (Figure 4). As noted above, the fans appear to have formed over an extended time period, so that it is unlikely that a local event such as a nearby impact or earthquake would have such long-lasting effects on fan formation.

[39] Variations in lithology are a possible contributor to the clustered pattern of fan development. Bolides impacting, for example, onto the margins of preexisting basins might have significant circumferential variations in wall lithology ranging, perhaps from fractured igneous rocks to loose sediment. One suggestive situation is the development of isolated fans on the two sides of the crater wall separating two impact basins (Fans E1 and E2 in Figure 11).

[40] We view climatic factors as a potentially strong control on the geography of fan development. Simulations of precipitation on Mars using global climate models show strong geographic control of location [Colaprete *et al.*, 2004]. The fan cluster at 30°W is located on the divide between Argyre and the eastern Valles Marineris chaos and outflow channels, including the Uzboi channel system that was active during the time period of fan development. The cluster at 290°W is on the flanks of the Hellas basin that may have hosted a deep, ice-covered lake [Moore and Wilhelms, 2001], and the central cluster at 335°W is at a topographic highpoint of the cratered highlands. The restriction of fan source areas to alcoves on the upper crater walls and the lack of apparent precipitation and fluvial incision on the fan surfaces may reflect microclimatic and orographic controls. Precipitation in mountainous terrain is strongly concentrated on local highs (e.g., moun-

tain peaks in the Basin and Range province typically receive >400 mm/yr, whereas basins often receive less than 100 mm/yr [Prudic *et al.*, 1995; Harrill and Prudic, 1998]). Thus upper crater walls should be favored for precipitation either as rain or snow. However, we find no evidence for universal association of fans with particular azimuths on the crater walls, which would be a strong indication of climatic control.

[41] The restriction of erosion and, possibly, runoff production, to specific alcoves on the crater walls may also reflect a positive feedback between alcove formation and local microclimate and hydrology. Steep basins enhance local mountain winds: updrafts in the afternoon and down-valley winds at night. These might interact with precipitation. In addition, for equivalent precipitation or snowmelt, runoff might be enhanced in the alcoves due to steep topography and exposed bedrock. Deeply incised basins are also sheltered from sunlight during low sun incident angles (e.g., winter and times of high obliquity), allowing the alcoves to cold-trap thick snow covers.

[42] The localized nature of the alcove erosion responsible for fans is possibly suggestive of erosion due to preferential groundwater emergence within the alcoves. Such a source of runoff has been suggested for the smaller and more recent gully systems on Mars [Malin and Edgett, 2000b]. However, the physiography of the alcoves and fans is not supportive of groundwater sources. The rims of the relatively undegraded craters supporting fans, being local topographic highs, are unlikely sources for large quantities of groundwater. Several of the fans extend from alcoves eroded into the septa rims between adjacent impacts (Fans M1, E1 and E2 in Figure 11). In particular, the alcoves supplying Fans E1 and E2 abut against each other at a narrow divide. It is also questionable that groundwater could supply discharge at a rate sufficient to transport coarse sediment and create sediment-transporting flows that would extend across tens of kilometers of fan surface.

[43] The lack of fan head trenching (exclusive of the fans in Holden), the fairly constant shapes and gradients, and the absence of changes in deposition centers on the fans of this study indicate that the last episodes of deposition occurred under a hydrological regime that was similar to that of its immediate predecessors. In other words, there is no evidence for a gradual decline in the final hydrological regime. By contrast, many if not most terrestrial fan systems show fan head trenching and translocation of deposition to the toe of the fans in response to changes from glacial to interglacial climate [e.g., Bull, 1991]. There is no further fluvial modification of fan surfaces of even a modest scale. These fans formed in a climate that very abruptly ended at least with respect to its ability to generate precipitation and runoff, something that is not seen on Earth. Equally noteworthy is the absence of evidence for antecedent fans of the slope, size and isolation of those of this study. Sediment deposits within mid-Noachian degraded craters are gentler (Figures 15 and 16), more concave (Figure 12), and derive from widespread dissection of the crater walls rather than incision of localized alcoves, resulting in planar rather than fan-shaped deposits. Indeed, some of the fans of this study have feeder valleys that incise preexisting smooth and presumably sediment-filled basins as they travel from their catchments (e.g., Bakhuisen, Holden), which otherwise

exhibit no nonfan dissection. Taken together, this may imply that the climate preceding the era of the study fans was also not conducive to generation of steep, large, and isolated alluvial fans.

[44] A climate that suddenly stops supporting fan formation and may have just as suddenly commenced seems unlikely to be the consequence of a gradual decline in Mars' ability to support an atmosphere-surface hydrologic cycle [e.g., Pollack *et al.*, 1987; Squyres and Kasting, 1994]. Perhaps better candidate climates are those ushered in by "cataclysmic" events that induce excursions from some steady state. If Mars had already evolved to a "steady state" climate that disfavored a hydrologic cycle conducive to the formation of this study's fans at the time we speculate that they were formed (at approximately the Noachian-Hesperian boundary), potential "cataclysmic" events that might induce sudden climate perturbations that have been dated to this time are outflow channels [e.g., Grant, 1987, 2000], large-scale volcanic eruptions [e.g., Scott and Carr, 1978; Tanaka, 1986], and large impacts [e.g., Tanaka, 1986; Hartmann and Neukum, 2001]. The ability of outflow channel flooding to induce a period of precipitation and runoff was called into question by Moore *et al.* [1995]. Several studies have proposed that the release of volatiles by large-scale volcanic events can bring on a hydrologic-cycle-conducive environment; however, these events are usually ascribed to a time well prior to the Hesperian [e.g., Phillips *et al.*, 2001].

[45] Carr [1989] and, more recently, Segura *et al.* [2002] have proposed that large impacts could induce a period of precipitation (and/or ground ice melt) and runoff. Even if individual impact-induced precipitation and runoff episodes do not persist long enough to form the fans of this study, the accumulation of the effects of many such events could. We searched for evidence (i.e., partially buried craters) of long ( $\sim 10^6$  year scale) hiatuses in fan growth but saw none. This, however, does not mean that hiatuses did not occur, as the last episode of fan deposits in combination with subsequent mantling could easily mask any such evidence. Also, the Segura *et al.* [2002] hypothesis, as it was originally presented, required impact events much larger than those that we have evidence took place at the Noachian-Hesperian transition. Recent modeling by this group [e.g., Colaprete *et al.*, 2004], however, indicates that impacts in the range of those seen to have taken place during the time of fan formation could produce several years to several decades of precipitation and runoff over a regional area. So, while the impact-induced climate change hypothesis looks promising, it does not explain why there was a long hiatus prior to the era of fan formation, as large impacts occurred throughout the Noachian.

#### 4. Future Work

[46] This study reports the observations of large alluvial fans on Mars, which have gone unrecognized until the acquisition of widespread 100 m/pixel imaging and global  $\sim 1$  km/pixel topographic data. Alluvial fans, along with one or two unambiguous fluvial deltas, represent the only distinctly recognizable constructional water-lain deposits on Mars identifiable exclusively from orbital data. However, this study could not be comprehensive, due to the

incomplete coverage of THEMIS daytime IR 100 m/pixel imaging that was utilized to survey fans at the time of its writing, and the self-imposed limits on the search area. Also, our dependence on MOLA data and the incomplete available THEMIS coverage may have introduced a recognition bias against small fans. We did not examine in detail the complex interaction of deposition and erosion among the fans and the Uzboi fluvial system within Holden crater, which might be diagnostic of fan evolution there. Also an investigation of the scaling relationships among surface gravity, particle sizes, flow properties, and fan geometries were beyond the purview of our study. As comprehensive data from THEMIS, and as especially high-resolution topographic data from the High Resolution Stereo Camera (HRSC) aboard Mars Express, become available, it will be possible to complete the survey of Martian fans, more precisely measure their properties, and infer their implication for Martian climate history.

[47] **Acknowledgments.** We thank Bill Dietrich and Adrian Harvey for their careful reviews. Thanks go to Carrie Chavez for her help with manuscript preparation and Pam Engebretson for her help with figure preparation. This research was performed under a grant from NASA's Mars Data Analysis Program.

#### References

- Beatty, C. B. (1970), Age and estimated rate of accumulation of an alluvial fan, White Mountains, California, U.S.A., *Am. J. Sci.*, **268**, 50–77.
- Beatty, C. B. (1974), Debris flows, alluvial fans, and a revitalized catastrophism, *Z. Geomorphol. Suppl.*, **21**, 39–51.
- Beatty, C. B. (1990), Anatomy of a White Mountain debris flow: The making of an alluvial fan, in *Alluvial Fans: A Field Approach*, edited by A. H. Rachocki and M. Church, pp. 69–90, John Wiley, Hoboken, N. J.
- Blair, T. C., and J. G. McPherson (1994), Alluvial fan processes and forms, in *Geomorphology of Desert Environments*, edited by A. D. Abrahams and A. J. Parsons, pp. 354–402, CRC Press, Boca Raton, Fla.
- Bull, W. B. (1962), Relations of alluvial-fan size and slope to drainage-basin size and lithology in western Fresno County, California, *U.S. Geol. Surv. Prof. Pap.*, **450-B**, 51–53.
- Bull, W. B. (1964), Geomorphology of segmented alluvial fans in western Fresno County, California, *U.S. Geol. Surv. Prof. Pap.*, **352E**, 89–129.
- Bull, W. B. (1972), Recognition of alluvial fan deposits in the stratigraphic record, in *Recognition of Ancient Sedimentary Environments*, edited by J. K. Rigby and W. K. Hamblin, *Spec. Publ. Soc. Econ. Paleontol. Mineral.*, **16**, 63–83.
- Bull, W. B. (1991), *Geomorphic Responses to Climatic Change*, 326 pp. Oxford Univ. Press, New York.
- Cabrol, N. A., and E. A. Grin (2001), The evolution of lacustrine environments on Mars: Is Mars only hydrologically dormant?, *Icarus*, **149**, 291–328.
- Carr, M. H. (1989), Recharge of the early atmosphere of Mars by impact-induced release of CO<sub>2</sub>, *Icarus*, **79**, 311–327.
- Christensen, P. R. (1986), Regional dust deposits on Mars: Physical properties, age, and history, *J. Geophys. Res.*, **91**(B3), 3533–3545.
- Colaprete, A., R. M. Haberle, T. L. Segura, O. B. Toon, and K. Zahnle (2004), The effect of impacts on the early Martian climate, in *Second Conference on Early Mars*, Abstract 8016, Lunar and Planet. Inst., Houston, Tex.
- Craddock, R. A., and A. D. Howard (2002), The case for rainfall on a warm, wet early Mars, *J. Geophys. Res.*, **107**(E11), 5111, doi:10.1029/2001JE001505.
- Crumpler, L. S., and K. L. Tanaka (2003), Geology and MER target site characteristics along the southern rim of Isidis Planitia, Mars, *J. Geophys. Res.*, **108**(E12), 8080, doi:10.1029/2002JE002040.
- Denny, C. S. (1965), Alluvial fans in the Death Valley region, California and Nevada, *U.S. Geol. Surv. Prof. Pap.*, **466**.
- Denny, C. S. (1967), Fans and pediments, *Am. J. Sci.*, **265**, 81–105.
- Eckis, R. (1928), Alluvial fans of the Cucamonga district, southern California, *J. Geol.*, **36**, 224–247.
- Goldspiel, J. M., and S. W. Squyres (1991), Ancient aqueous sedimentation on Mars, *Icarus*, **89**, 392–410.

- Grant, J. A. (1987), The geomorphic evolution of eastern Margaritifer Sinus, Mars, in *Advances in Planetary Geology, NASA Tech. Memo., 89871*, 1–268.
- Grant, J. A. (2000), Valley formation in Margaritifer Sinus, Mars, by precipitation-recharged ground-water sapping, *Geology*, *28*, 223–226.
- Greeley, R., and J. E. Guest (1987), Geologic map of the eastern equatorial region of Mars, *U.S. Geol. Surv. Misc. Invest. Ser., Map I-1802-B*.
- Hack, J. T. (1960), Interpretation of erosional topography in humid temperate regions, *Am. J. Sci.*, *258-A*, 89–97.
- Hack, J. T. (1965), Geomorphology of the Shenandoah Valley, Virginia and West Virginia, and origin of residual ore deposits, *U.S. Geol. Surv. Prof. Pap.*, *484*.
- Harrill, J. R., and D. E. Prudic (1998), Aquifer systems in the Great Basin region of Nevada, Utah, and adjacent states—Summary report, *U.S. Geol. Surv. Prof. Pap.*, *1409-A*.
- Hartmann, W. K., and G. Neukum (2001), Cratering chronology and the evolution of Mars, *Space Sci. Rev.*, *96*(1/4), 165–194.
- Harvey, A. M. (1990), Factors influencing quaternary alluvial fan development in southeast Spain, in *Alluvial Fans: A Field Approach*, edited by A. H. Rachocki and M. Church, pp. 109–129, John Wiley, Hoboken, N. J.
- Harvey, A. M. (1997), The role of alluvial fans in arid zone fluvial systems, in *Arid Zone Geomorphology: Process, Form and Change in Drylands*, 2nd ed., edited by D. S. G. Thomas, pp. 231–259, John Wiley, Hoboken, N. J.
- Head, J. W., J. F. Mustard, M. A. Kreslavsky, R. E. Milliken, and D. R. Marchant (2003), Recent ice ages on Mars, *Nature*, *426*, 797–802, doi:10.1038/02114.
- Hooke, R. L. B. (1967), Processes on arid-region alluvial fans, *J. Geol.*, *75*, 438–460.
- Hooke, R. L. B. (1968), Steady-state relationships on arid-region alluvial fans in closed basins, *Am. J. Sci.*, *266*, 609–629.
- Howard, A. D. (1980), Thresholds in river regimes, in *Thresholds in Geomorphology*, edited by D. R. Coates and J. D. Vitek, pp. 227–258, Allen and Unwin, St Leonards, NSW, Australia.
- Howard, A. D. (1994), A detachment-limited model of drainage-basin evolution, *Water Resour. Res.*, *30*, 2261–2285.
- Howard, A. D., and R. Craddock (2000), Degraded Noachian craters: Fluvial versus lava infilling, *Lunar and Planetary Sci.*, *XXXI*, abstract 1542.
- Howard, A. D., and J. M. Moore (2004a), Scarp-bounded benches in Gorgonum Chaos, Mars: Formed beneath an ice-covered lake?, *Geophys. Res. Lett.*, *31*, L01702, doi:10.1029/2003GL018925.
- Howard, A. D., and J. M. Moore (2004b), Changing style of erosion during the Noachian-Hesperian transition and a possible climatic optimum, *Lunar Planet. Sci.*, *XXXV*, Abstract 1192.
- Kochel, R. C. (1990), Humid fans of the Appalachian Mountains, in *Alluvial Fans: A Field Approach*, edited by A. H. Rachocki and M. Church, pp. 109–129, John Wiley, Hoboken, N. J.
- Komar, P. D. (1980), Modes of sediment transport in channelized water flows with ramifications to the erosion of the Martian outflow channels, *Icarus*, *42*, 317–329.
- Lece, S. A. (1990), The alluvial fan problem, in *Alluvial Fans: A Field Approach*, edited by A. H. Rachocki and M. Church, pp. 3–24, John Wiley, Hoboken, N. J.
- Lustig, L. K. (1965), Clastic sedimentation in Deep Springs Valley, California, *U.S. Geol. Surv. Prof. Pap.*, *352-F*, 131–192.
- Mack, G. H., and M. R. Leeder (1998), Channel shifting of the Rio Grande, southern Rio Grande Rift: Implications to alluvial stratigraphic models, *Sediment. Geol.*, *117*, 207–219.
- Malin, M. C., and K. S. Edgett (2000a), Sedimentary rocks of early Mars, *Science*, *290*, 1927–1937.
- Malin, M. C., and K. S. Edgett (2000b), Evidence for recent groundwater seepage and surface runoff on Mars, *Science*, *288*, 2330–2335.
- Malin, M. C., and K. S. Edgett (2003), Evidence for persistent flow and aqueous sedimentation on early Mars, *Science*, *302*, 1931–1934.
- Moore, J. M. (1990), Nature of the mantling deposit in the heavily cratered terrain of northeastern Arabia, Mars, *J. Geophys. Res.*, *95*, 14,279–14,289.
- Moore, J. M., and A. D. Howard (2004), Large well-exposed alluvial fans in deep Late-Noachian craters, *Proc. Lunar Planet. Sci. Conf. 35th*, Abstract 1443.
- Moore, J. M., and D. E. Wilhelms (2001), Hellas as a possible site of ancient ice-covered lakes on Mars, *Icarus*, *154*, 258–276.
- Moore, J. M., G. D. Clow, W. L. Davis, V. C. Gulick, D. R. Janke, C. P. McKay, C. R. Stoker, and A. P. Zent (1995), The Circum-Chryse region as a possible example of a hydrologic cycle on Mars: Geologic observations and theoretical evaluation, *J. Geophys. Res.*, *100*, 5433–5447.
- Moore, J. M., A. D. Howard, W. E. Dietrich, and P. M. Schenk (2003), Martian Layered Fluvial Deposits: Implications for Noachian Climate Scenarios, *Geophys. Res. Lett.*, *30*(24), 2292, doi:10.1029/2003GL019002.
- Phillips, R. J., et al. (2001), Ancient geodynamics and global-scale hydrology on Mars, *Science*, *291*(5513), 2587–2591.
- Pieri, D. C. (1980), *Geomorphology of Martian Valleys*, 362 pp., Natl. Aeron. and Space Admin., Washington, D. C.
- Pollack, J. B., J. F. Kasting, S. M. Richardson, and K. Poliakov (1987), The case for a wet, warm climate on early Mars, *Icarus*, *71*, 203–224.
- Pondrelli, M., A. Baliva, S. di Lorenzo, L. Marinangeli, and A. P. Rossi (2004), Complex evolution of paleoclastrine systems on Mars: An example from the Holden Crater, *Proc. Lunar Planet. Sci. Conf. 35th*, Abstract 1249.
- Prudic, D. E., J. R. Harrill, and T. J. Burbey (1995), Conceptual evaluation of regional ground-water flow in the carbonate-rock province of the Great Basin, Nevada, Utah, and adjacent states, *U.S. Geol. Surv. Prof. Pap.*, *1409-D*.
- Schumm, S. A., and R. W. Lichty (1965), Time, space and causality in geomorphology, *Am. Sci.*, *263*, 110–119.
- Scott, D. H., and M. H. Carr (1978), Geologic map of Mars, *U.S. Geol. Surv. Misc. Invest. Ser., Map I-1083*.
- Scott, D. H., and K. L. Tanaka (1986), Geologic map of the western equatorial region of Mars, *U.S. Geol. Surv. Misc. Invest. Ser., Map I-1802-A*.
- Segura, T. L., O. B. Toon, A. Colaprete, and K. Zahnle (2002), Environmental effects of large impacts on Mars, *Science*, *298*, 1977–1980.
- Soderblom, L. A., T. J. Kreidler, and H. Masursky (1973), Latitudinal distribution of a debris mantle on the Martian surface, *J. Geophys. Res.*, *78*(20), 4117–4122.
- Squyres, S. W., and J. F. Kasting (1994), Early Mars: How warm and how wet?, *Science*, *265*, 744–748.
- Tanaka, K. L. (1986), The stratigraphy of Mars, *Proc. Lunar Planet. Sci. Conf. 17th*, Part 1, *J. Geophys. Res.*, *91*, suppl., E139–E158.
- Williams, R. M. E., K. S. Edgett, and M. C. Malin (2004), Young fans in an equatorial crater in Xanthe Terra, Mars, *Proc. Lunar Planet. Sci. Conf. 35th*, abstract 1415.

A. D. Howard, Department of Environmental Sciences, University of Virginia, Box 400123, Charlottesville, VA 22904, USA. (ah6p@virginia.edu)

J. M. Moore, Space Sciences Division, NASA Ames Research Center, MS 245-3, Moffett Field, CA 94035, USA. (jeff.moore@nasa.gov)